Increased sexual dimorphism evolves in a fossil stickleback following ecological release from fish piscivores

Allison Ozark[1,*], Matthew Stuart[2,3,*], Raheyma Siddiqui[1], Akhil Ghosh[2,3]
Samantha Swank[1], Michael A. Bell[4], Gregory J. Matthews[2,3], and Yoel E. Stuart[1,+]

[1] Department of Biology, Loyola University Chicago, Chicago, IL, USA
[2] Department of Mathematics and Statistics, Loyola University Chicago, Chicago, IL, U
[3] Center for Data Science and Consulting, Loyola University Chicago, Chicago, IL, U
[4] University of California Museum of Paleontology, Berkeley, CA, USA
[*] Equal contribution
[+] Corresponding: ystuart@luc.edu

Abstract

Everyone loves the stickle

Keywords: Stickle

1 Introduction

Ecological release theory suggests that a prey population's niche should expand when predation is relaxed or removed, as prey take advantage of new enemy free space (reviewed in Herrmann, Stroud, and Losos (2021)). Niche expansion could manifest through a combination of increasing within- and between-individual niche widths (Bolnick et al. (2010); Herrmann, Stroud, and Losos (2021)), including divergence between the sexes (Bolnick and Doebeli (2003); Cooper, Gilman, and Boughman (2011)). Theory and empirical data suggest that a population presented with ecological opportunity following ecological release might experience disruptive selection on males and females stemming from intraspecific competition over newly accessible resources, resulting in intersexual divergence in habitat use (W. (1968); Shine (1989); Bolnick and Doebeli (2003); Butler, Sawyer, and Losos (2007); Bolnick and Lau (2008); Cooper, Gilman, and Boughman (2011); but see Stuart et al. (2021); Blain (2022)). Accordingly, sexes should also diverge in morphological traits associated with habitat use; such ecologically-driven "character displacement between the sexes" is therefore one explanation for phenotypic sexual dimorphism (S. P. De Lisle and Rowe (2015); S. Paiva De Lisle S. P. and Rowe (2018)).

We tested this link between release from predators and the evolution of sexual dimorphism in a well-preserved, finely-resolved, ~16,000 year-long sequence of the fossil stickleback fish (Gasterosteus doryssus). The fossil lineage appeared in the depositional environment as a fully armored form, with complete pelvic girdles, two pelvic spines, and three dorsal spines, on average (Michael A. Bell, Travis, and Blouw (2006); Stuart, Travis, and Bell (2020)). However, this habitat appears to have been missing fish piscivores (e.g., trout and other salmonids known to prey on modern stickleback; M. A. Bell (2009)), relaxing putative selection for armor (T. E. Reimchen (1980), T. E. Reimchen (1994), O. Bell M. A. and Koenings (1993); Bowne (1994); Roesti and Schluter (2023)). The lineage adaptively evolved armor loss but also reduction in the means of several other traits (Hunt, Bell, and Travis (2008); Stuart, Travis, and Bell (2020); Siddiqui et al. in prep). In particular, tooth wear data suggest that the population shifted to eat more planktonic prey through time, indicative of increased open water habitat use (Purnell et al. 2007). If this divergence in habitat use is partitioned between sexes (Reimchen T. E. and Nosil (2004); Spoljaric and Reimchen (2008);D. S. Reimchen T. E. (2016)), then we should expect sexual dimorphism to evolve for traits related to habitat use in G. doryssus.

To test this prediction, we imputed the sex of individual fossils, which is unobserved in practice, with Multiple Imputation by Chained Equations (MICE) (Buuren and Groothuis-Oudshoorn (2011)), using observed data from extant stickleback of known sex to train the imputation model. Then we tracked the multivariate evolution of sexual dimorphism over ~16,000 years for 16 traits related to swimming, feeding and defense.

2 Methods and Materials

A major challenge in this work is inferring the sex of fossil stickleback specimens. Indeed, for most species, sex cannot be detected directly, except for lineages whose sexes are distinguished by the presence or absence of sex-specific characters (Hone and Mallon (2017); Saitta et al. (2020)). Instead, paleobiologists resort to statistical detection of sex and sexual dimorphism, including tests for bimodality in trait distributions (e.g., Hone and Mallon (2017)) and divergence in growth curves (e.g., Saitta et al. (2020)). We used a third approach to infer fossil sex and study the evolution of sexual dimorphism by taking advantage of the fact that G. doryssus is part of the extant threespine stickleback species complex, Gasterosteus aculeatus. We measured the same trait set from a phenotypically diverse set of extant G. aculeatus populations, for whom individual sex was known. We then combined fossil and extant data sets, treated fossil sex as missing data, and used the MICE (Buuren and Groothuis-Oudshoorn (2011)) multiple imputation (Little and Rubin (2002)) algorithm, and implemented in R (Team (2022)), to impute individual sex of the fossil data set 100 times. We then fit a modified Ornstein–Uhlenbeck (OU) (Uhlenbeck and Ornstein (1930)) model using a Bayesian framework to the data to test for the evolution of sexual dimorphism in each trait.

3 Data

3.1 Fossil Specimen Data

We used Gasterosteus doryssus data that were previously reported by Stuart, Travis, and Bell (2020), Voje, Bell, and Stuart (2022), and Siddiqui et al. (in review). Briefly, the data were collected from fossil Series K from Quarry D (Cerasoni et al., in review), dug from an open pit diatomite mine at 9.526° N, 119.094° W, near Fernley, Nevada, USA. Series K consisted of 18 samples taken at ~1000-year intervals, and mean sample times span ~16,363 years. Fish from series K were measured for 16 ecomorphological traits related to armor, swimming, and feeding (Table 1). Series K started at a previously documented horizon when a low armored lineage of stickleback with zero to one dorsal spines, zero pelvic spines, and highly reduced pelvises was completely replaced by a high armored lineage of stickleback with three dorsal spines, two pelvic spines, and complete (Bell et al. 2006; Bell 2009; Stuart et al. 2020). This lineage subsequently evolved reduction in armor, body size, and traits related to swimming and feeding (Bell et al. 2006; Stuart et al. 2020; Siddiqui et al. in review). The tempo and mode of armor reduction during this sequence suggests adaptive evolution by natural selection (Hunt et al. 2008), and we focus on the multivariate evolution of sexual dimorphism by this second lineage.

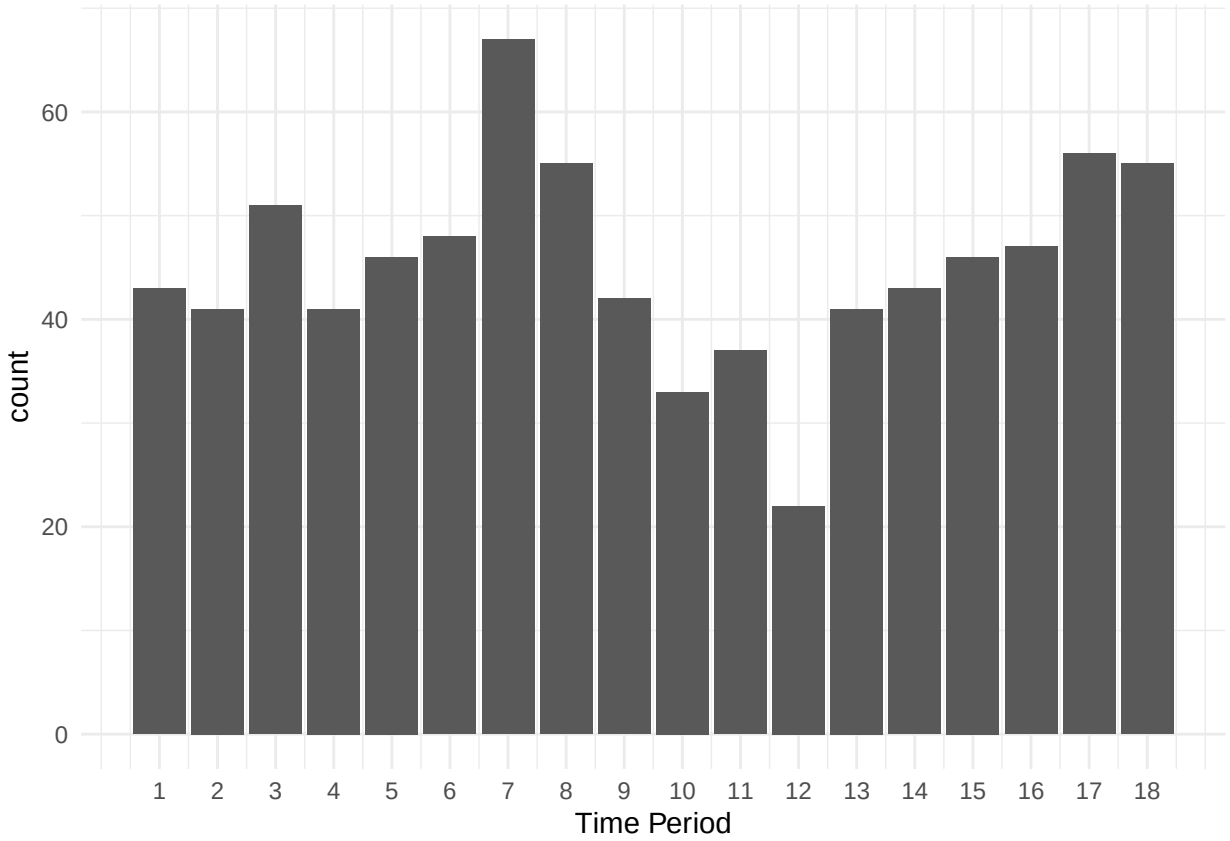

Figure 1: Fossil sampel size for each time period

The fossil data consists of 814 specimens with unknown sex over 18 time periods spaced ~1000 years apart. Figure 1 shows the sample size at each of the 18 time periods. There are at least 22 specimens at each time period with a high of 67 specimens in period 7.

Table 1: Traits and trait descriptions. 'sc' denotes size correction of trait against standard length. Names of bones follow Bowne (1994) unless otherwise noted.

Trait Name	Trait Code	Trait Description
Standard Length	`stl`	Distance from anterior tip of premaxilla to posterior end of last vertebra (hypural plate)
Dorsal Spine	`mds`	Number of dorsal spines from 0 to 3
Dorsal Fin Ray	`mdf`	Number of bones in the dorsal fin posterior to the third dorsal spine (i.e., soft dorsal fin rays)

Trait Name	Trait Code	Trait Description
Anal Fin Ray	`maf`	Number of bones in the anal fin posterior to the anal spine (i.e., soft dorsal fin rays)
Abdominal Vertebra	mav	Number of vertebrae anterior to the first vertebra contacting an anal fin pterygiophore (Aguirre et al. 2014)
Caudal Vertebra	`mcv`	Number of vertebrae posterior to and including the first vertebra contacting an anal fin pterygiophore (Aguirre et al. 2014)
Pterygiophore number	`mpt`	Number of pterygiophores anterior to but excluding the pterygiophore under the third dorsal spine, which is immediately anterior to and contiguous with the dorsal fin
Pelvic Spine length	`lps.sc`	Length from the base of one pelvic spine above its articulation with the pelvic girdle to its distal tip
Ectocoracoid	`ect.sc`	Length between the anterior and posterior tips of the shoulder girdle base (i.e., ectocoracoid)
Pelvic Girdle	`tpg.sc`	Length between the anterior to posterior tips along midline. If vestigial, the sum of longest anterior-posterior axis for the vestiges
Cleithrum length	`cle.sc`	Length from free dorsal tip to ventral tip of the cleithrum on the anterior margin of the shoulder girdle (i.e., cleithrum)
Premaxilla	`pmx.sc`	Length from the anterior tip of the premaxilla to the distal tip of the ascending process of the premaxilla
Dorsal Spine	`Ds#.sc# = 1,2,or 3`	Length from the base of a dorsal spine above the pterygiophore to its distal tip along the anterior edge

Trait Name	Trait Code	Trait Description
Pterygiophore	`lpt.sc`	Distance between the anterior to posterior tips of the pterygiophore immediately preceding the 3rd dorsal spine (when present)

3.2 Extant Specimen data

To span the gamut of stickleback diversity for our predictive model, we sampled modern stickleback from lakes containing generalist stickleback populations (Hendry et al. (2009); Bolnick (2011)) and from lakes containing benthic-limnetic species pairs (Baumgartner et al. 1988; Schluter and McPhail (1992)) (Table 2 (What is this?)). The generalist populations were collected by YES in 2013 and previously described in Stuart et al. (2017). These samples were fixed in formalin, then stained for bone with Alizarin Red in 2013. Benthic and limnetic specimens were kindly loaned by D. Schluter and his lab at University of British Columbia. They collected benthic and limnetic individuals from Enos Lake in 1988 and from Emily Lake, Little Quarry Lake, Paxton Lake, and Priest Lake in 2018. The Enos specimens had been fixed whole in formalin and stored in 40% isopropanol. The specimens from the other lakes were initially preserved whole in 95% ethanol in the field before being gradually transferred to water then formalin in the lab and ultimately stored in 40% isopropanol. In 2019, we stained these specimens for bone using Alizarin Red.

We next replicated fossil data collection (Table 1) on these extant specimens. Standard length as well as pelvic-spine length on each side were measured with calipers. We used a dissection microscope to count dorsal spines, pelvic spines, dorsal-fin rays, and anal-fin rays. Right and left-side pelvic girdle lengths and ectocoracoid lengths were measured from ventral photographs taken using a Canon EOS Rebel T7 with a Tamron 16-300 mm MACRO lens mounted on a leveled Kaiser RS1 copy stand. Specimens were held in place for ventral photographs using a small tabletop vise with an attached scale bar. Lateral X-rays were used to measure dorsal spine length, number of pterygiophores anterior to the pterygiophore holding the third spine, length of the pterygiophore just anterior to the third spine, cleithrum length, and pre-maxilla ascending branch length. We also counted vertebrae from the X-rays: abdominal vertebrae were counted anterior to the first vertebra with a haemal spine contacting an anal fin pterygiophore. Caudal vertebrae were posterior, including the first vertebra with the haemal spine contacting the anal fin pterygiophore (following Aguirre, Walker, and Gideon (2014). X-rays were taken with an AXR Hot Shot X-ray Machine (Associated X-ray Corporation) at the Field Museum of Natural History. Specimens were exposed at 35kV and 4mA. Small fish were exposed for 7s, medium fish for 8s, and large fish

for 10s. We developed the film and scanned individual images of each fish using the B&W Negatives setting on an Epson Perfection 4990 Photo flatbed at 2400 dpi. Measurements from photographs and X-rays were taken with FIJI (Schindelin et al. 2012) and its plugin ObjectJ (https://sils.fnwi.uva.nl/bcb/objectj/). All photographs, X-rays, and ObjectJ files have been uploaded to Morphosource.org (accession # TBD). We dissected individuals from the generalist populations to determine sex from the gonads. Individuals from the species-pair lakes were sexed by Schluter and his lab, using a genotyping protocol (confirm and cite).

The extant data used here consists of a total of 367 specimens all with known sex. Of these, there are 202 and 165 female and male specimens, respectively.

3.3 Outlier analysis.

To check for outliers, we calculated within-group means and standard deviations for each trait separately for K series fossil specimens (pooled across samples) and for extant specimens (pooled across lakes). We noted trait values greater than 3.5 standard deviations from the mean as potential outliers. We checked whether these potential outliers were a result of data entry and collection error and corrected them if they were. We turned the remaining outlier trait values to NAs. (confirm) (Wait, what? Why? Anything that was 3.5 SD above the mean was recorded as missing? How do you justify this?)

Missing data imputation, including fossil sex

Quantification and evolution of sexual dimorphism

What covariates do we have in the data: length, what else,

4 Models

4.1 Imputation Model

Let $\boldsymbol{W}$ be an $(n_{extant} + n_{fossil}) \times 1$ vector of the covariate gender of the stickleback fish and $\boldsymbol{Y}$ be an $(n_{extant} + n_{fossil}) \times K$ matrix of the K phenotypes of interest. Because the gender of the fossilized stickleback fish is unobservable, we further define $\boldsymbol{W} = (\boldsymbol{W}_{extant}^T, \boldsymbol{W}_{fossil}^T)^T$ where $\boldsymbol{W}_{extant}$ and $\boldsymbol{W}_{fossil}$ are the $n_{extant} \times 1$ and $n_{fossil} \times 1$ vectors of the observed extant gender and missing fossil gender, respectively.

We impute the missing gender for the fossil data by sampling from the posterior predictive distribution $P(\boldsymbol{W}_{fossil} | \boldsymbol{W}_{extant}, \boldsymbol{Y})$ using the multiple imputation by chained equations

(MICE) algorithm (Buuren and Groothuis-Oudshoorn (2011)) with predictive mean matching. Traditionally, the choice for the number of completed dats sets is a relatively small number such as $M = 5$ or $M = 10$. However, Zhou and Reiter (2010) recommend a larger number of imputed data sets if the data users intend on performing Bayesians analysis after imputation, which in this case, we do. Therefore, the imputation algorithm is run to obtain a total of $M = 100$ completed datasets. In addition to this, Zhou and Reiter (2010) suggests rather than using Rubin's combining rules to combine across imputed data sets, instead pool all of the draws from the posterior distributions across all of the imputed data sets to estimate the posterior distributions of parameters of interest. We proceed with our Bayesian analysis in this manner.

Akhil's stuff about validating the imputation model goes here.

4.2 Completed Data Model

We should note somewhere that we are only using the W_{fossil} in the modeling part. We drop the W_{extant}. So just note that W_{ti} is really $W_{fossil,ti}$. Not sure how to say this, but we need to make it clear that we are only using the fossil data for the OU modeling. Greg, check and see if this makes sense.

I think we need to move a lot of these details to the appendix.

For a given imputed dataset, let W_{ij} be the imputed gender and $\boldsymbol{Y}_{ij}$ be the $K \times 1$ vector of phenotypes for stickleback fossil j at time t_i where $i = 1, \ldots, T$ and $j = 1, \ldots, n_t$. Note, we are inputting only the fossil data into our model; connecting to the previous section, W_{ij} and $\boldsymbol{Y}_{ij}$ can be interpretted as $W_{fossil,ij}$ and $\boldsymbol{Y}_{fossil,ij}$. In addition, we denote $Y_{K,ij}$, the last variable in $\boldsymbol{Y}_{ij}$, to be the standard length of the fish,

$$Y_{K,ij} \overset{iid}{\sim} \begin{cases} \mathcal{N}(\mu_{K,ft_i}, \quad \sigma_K^2), & W_{ij} = \text{Female} \\ \mathcal{N}(\mu_{K,mt_i}, \quad \sigma_K^2), & W_{ij} = \text{Male} \end{cases} . \tag{1}$$

It is reasonable to assume that the other continuous traits of stickleback fish will have some correlation with its standard length **(CITATION)**. We account for this by adding an additional parameter, γ_k, into our model. More specifically, if $Y_{k,ij}$ is a continuous trait, then

$$Y_{k,ij} \overset{iid}{\sim} \begin{cases} \mathcal{N}(\mu_{k,ft_i} + \gamma_k Y_{K,ij}, \sigma_k^2), & W_{ij} = \text{Female} \\ \mathcal{N}(\mu_{k,mt_i} + \gamma_k Y_{K,ij}, \sigma_k^2), & W_{ij} = \text{Male} \end{cases} . \tag{2}$$

If $Y_{k,ij}$ is a discrete trait, the conventional method of modelling this data is by fitting a Poisson distribution. However, the Poisson distribution assumes that the mean and variance of $Y_{k,ij}$ are equal ($E(Y_{k,ij}) = \text{Var}(Y_{k,ij})$), while the empirical fossil data may have variances that are

smaller than their respective means. To combat this issue, we propose to fit the discrete traits to a generalized Poisson model as defined in (**GeneralizedPoisson?**). Specifically, if $X \sim GP(\lambda, \alpha)$, then

$$P(X = x) = \begin{cases} \frac{(1-\alpha)\lambda[(1-\alpha)\lambda+\alpha x]^{x-1}\exp\{-((1-\alpha)\lambda+\alpha x)\}}{x!} & (1-\alpha)\lambda + \alpha x \geq 0 \\ 0 & (1-\alpha)\lambda + \alpha x < 0 \end{cases}, \tag{3}$$

where $E(X) = \lambda$ and $Var(X) = \frac{\lambda}{(1-\alpha)^2}$. If $\alpha > 0$, then the variance is greater than the mean, called overdispersion; if $\alpha < 0$, then the variance is greater than the mean, called underdispersion; if $\alpha = 0$, then the model degenerates to a Poisson distribution.

We will use the generalized Poisson to model all of the discrete traits in our dataset. In addition, we assume that the discrete traits abdominal vertebrae (mav) and caudal vertebrae (mcv) also have correlation with the standard length of the fish (**CITATION**). If $Y_{k,ij}$ is one of the above traits, then

$$Y_{k,ij} \sim \begin{cases} GP(\exp\{\mu_{k,ft_i} + \gamma_k Y_{K,ij}\}, \alpha_k), & W_{ij} = \text{Female} \\ GP(\exp\{\mu_{k,mt_i} + \gamma_k Y_{K,ij}\}, \alpha_k), & W_{ij} = \text{Male} \end{cases}. \tag{4}$$

For the other discrete traits, we also assume the above model except we set $\gamma_k = 0$ because of the assumption of no correlation between the standard length and these traits. More specifically, we assume

$$Y_{k,ij} \sim \begin{cases} GP(\exp\{\mu_{k,ft_i}\}, \alpha_k), & W_{ij} = \text{Female} \\ GP(\exp\{\mu_{k,mt_i}\}, \alpha_k), & W_{ij} = \text{Male} \end{cases}. \tag{5}$$

In the above model descriptions, μ_{k,ft_i} and μ_{k,mt_i} model the time-t_i specific mean of phenotype k for female and male stickleback fish, respectively. We point out that, for the discrete traits, the means are represented by $\exp\{\mu_{k,ft_i}\}$ and $\exp\{\mu_{k,mt_i}\}$ for ease of use in our modeling technique. We further set

$$\mu_{k,gt_i} = \beta_{0,kg} + \beta_{1,kg} t_i + u_{k,gt_i}, \tag{6}$$

for $g \in \{f, m\}$ where $\beta_{0,kg}$ and $\beta_{1,kg}$ are regression parameters of phenotype Y_k for each gender, accounting for the possibility of a time-dependent trend in the mean structure, and u_{k,gt_i} is the corresponding residual. To account for potential correlations between the residuals for a given trait k and gender g, we fit an Ornstein-Uhlenback (OU) process (Uhlenbeck and Ornstein (1930)). More specifically, define $du_{k,gt} = u_{k,g(t+dt)} - u_{k,gt}$, the change in u_k, gt for

a given trait k and gender g over a miniscule time period dt. The OU process is defined as

$$du_{k,gt} = -\kappa_k u_{k,gt} dt + \tau_k dW_t, \tag{7}$$

where κ_k is a parameter associated with the correlation between $u_{k,gt}$ and $u_{k,g(t+dt)}$, τ_k is the standard deviation of the OU process, and W_t is a standard Brownian motion. As shown in Uhlenbeck and Ornstein (1930), the closed form solution for the SDE in (7) is

$$u_{k,gt_i} \overset{iid}{\sim} \mathcal{N}\left(u_{k,gt_{i-1}} \exp\{-\kappa_k(t_i - t_{i-1})\}, \frac{\tau_k^2(1 - \exp\{-2\kappa_k(t_i - t_{i-1})\})}{2\kappa_k}\right) \tag{8}$$

for $i = 2, \cdots, T$. In a traditional OU process, the initial value u_{k,gt_1} is assumed to be a (potentially unknown) constant, and we discuss the procedure for estimating this value below.

In our empirical study, we analyze the following four nested models for the mean process outlined in (6):

- OU with Trend: The mean process for each phenotype $k = 1, \cdots, K$ and $g \in \{f, m\}$ as previously defined.
- OU with No Trend: No linear trend on the mean processes and the overall mean of the phenotype is constant for each gender. This is achieved by setting $\beta_{1,kg} = 0$ in (6) for $k = 1, \cdots, K$ and $g \in \{f, m\}$
- No OU with Trend: No random fluctuations on the mean processes, i.e. the OU process assumption is not needed. This is achieved by setting $u_{k,gt_i} = 0$ in (6) for $k = 1, \cdots, K$, $g \in \{f, m\}$, and $i = 1, \cdots, T$.
- No OU with No Trend: The mean for a specific trait and specific gender at each time point is a constant value. This is achieved by setting $\beta_{1,kg} = 0$ and $u_{k,gt_i} = 0$ in (6) for $k = 1, \cdots, K$, $g \in \{f, m\}$, and $i = 1, \cdots, T$.

Because we are fitting a dataset with a stochastic structure on the means of the phenotypes, and we are interested in the distribution of the overall structure of these means, we analyze the data via a Bayesian analysis. Bayesian data analysis is also more naturally used when we have to impute data (**CITATION**). To aid in the sampling procedure for the discrete phenotypes, we declare

Priors: To aid in the sampling procedure for the discrete phenotypes, we declare $\phi_k = \log\left(\frac{\alpha_k - \max_{i,j}(-\lambda_{k,ij}/y_{k,ij})}{1-\alpha_k}\right)$ where $\lambda_{k,ij} = \begin{cases} \exp(\mu_{k,ft_i} + \gamma_k Y_{K,ij}) & W_{ij} = \text{Female} \\ \exp(\mu_{k,mt_i} + \gamma_k Y_{K,ij}) & W_{ij} = \text{Male} \end{cases}$. This transformation is performed to ensure our algorithm can properly sample from the posterior distribution of interest.

For $k = 1, \cdots, K$,

$$
\begin{aligned}
u_{k,gt_1} &\overset{iid}{\sim} \mathcal{N}(0, \tau_{0,k}) \\
\sigma_k &\overset{iid}{\sim} \mathcal{N}(0, 10) I_{\{\sigma > 0\}} \\
\sigma_k &\overset{iid}{\sim} \mathcal{N}(0, 10) \\
\tau_k &\overset{iid}{\sim} \mathcal{N}(0, 10) I_{\{\tau > 0\}} \\
\tau_{0,k} &\overset{iid}{\sim} \mathcal{N}(0, 20) I_{\{\tau > 0\}} \\
\kappa_k &\overset{iid}{\sim} \mathcal{N}(0, 1) I_{\{\kappa_g > 0\}} \\
\gamma_k &\overset{iid}{\sim} \mathcal{N}(0, 5) \\
\beta_{0,kg} &\overset{iid}{\sim} \mathcal{N}(0, 100) \\
\beta_{1,kg} &\overset{iid}{\sim} \mathcal{N}(0, 3)
\end{aligned}
\tag{9}
$$

We also note that, for the discrete phenotypes in equations (4) and (5), there is no σ_k, and is not sampled, and for the continuous phenotypes in equation (2), there is no ϕ_k and is not sampled.

All models were built using Team (2022) and (**S**TAN)

Cornuault (2022) Bayesian OU model.

5 Results

As previously described, four models for the mean process were considered for each trait. Within each trait, the model with the lowest DIC was chosen for that train. All subsequent results presented here use the model with the lowest DIC individually by trait. Table 5.1 shows the model that was selected for each trait. About half of the traits had models with a trend, and most models did not include an OU component. The traits that did include an OU component were caudal vertebra (mcv), pelvic spine lentgh (lpt), abdominal vertebra (mav), and standard length (stl) with caudal vertebra (mcv) being the only model with both a trend and an OU component. This implies that not only does caudal vertebra size have a linear trend across gender, but the average size at one time period is highly correlated with the average size at the next time period.

	OU	No OU
Trend	mcv	ds2, ds3, ect, maf, mdf
No Trend	lpt, mav, stl	cle, ds1, lps, pmx

5.1 Best fitting models

5.2 Sexual Dimorphism

Table **??** shows the posterior probability of the differences in the means between male and female specimens at each time point. Probabilities near 0.5 indicate very little difference in the means whereas probabilities far from 0.5 indicate sexual dimorphism with values of 0 and 1 indicating larger mean values for females and males, respectively. These results are shown graphically in figure 3.

Figure 2 shows the posterior mean difference for males versus females (values above 0 indicate means that were greater for males versus females). The full poosterior distributions over time for all traits are shown in the appendix.

Traits such as standard length (stl), anal fin ray (maf), dorsal fin ray (mdf), premaxilla (pmx), and dorsal spine 1 (ds1) demonstrate constant sexual dimorphism with all but the last having learger mean values in male sepcimen. Other traits such as abdominal vertebra (mav), caudal vertebra (mcv), and pelvic spine length (lps) don't appear to have any discernable sexual dimorphism in the means. Dorsal spine 3 (ds3) exhibits sexual dimorphism that changes over time. The mean number of dorsal spine 3 begins larger for females for the earliest observed time periods. Over time, however, this switches and the male specimens exhibit larger mean values for the latest observed time periods.

5.3 Changes over time

Table **??** shows the probability that the posterior distribution of the differences in the mean is greater than the posterior distribution of the differences at the first time point. Values near 0.5 indicate very little difference between the distributions whereas values closer to 0 and 1 indicate changes in the distributions with values of 1 meaning the difference in means has shifted towards males having a larger mean and values of 0 indicating the difference in means has shifted towards larger means in females. These results are shown graphically in figure 4.

The amount of sexual dimporphism over time does not change substantially for a majority of the trait observed here (i.e. cle, ds1, ds2, ect, lps, lpt, mav, mcv, pmx, stl). Traits that trend away from the mean difference at the first observed time point include dorsal spine 3 (ds3), anal fin ray (maf), and dorsal fin ray (mdf).

The posterior mean of the mean number of dorsal spine rays at the first observed time point is 2.29 for males and for females it is 2.45. At the last observed time point, the average number for males and female both dropped to 1.265 and 1.185 for males and females, respectively. This resulted in a mean number of dorsal spine 3 lost by males of 1.027 and for females it was 1.264. This resulted in a change of the mean difference from time point 1 to time point 18 of 0.236. Basically, males and females both lowered the mean number of dorsal spine 3, but females lowered their mean more than the males.

We also observed a change in the differences between males and females for the number of bones int he anal fin ray (maf) and the number of bones in the dorsal fin ray. The difference in the means of males versus females for anal fin ray bones changed by 0.152 over the course of the observed time periods. This change was driven mostly by the change in females. At the first observed time period the had on average 8.291 bones dropping to 8.170 over the 18 times periods observed. Whereas for males the change in means rose only from 8.518 to 8.549, about 0.0316 bones on average.

A similar change in the difference of the means over time was observed for the number of bones in the dorsal fin (mdf). However, unlike maf, this change in sexual dimporhism was driven entirely by the males. The mean change for females over the 18 observed time periods was only 0.0055 with the average number of dorsal fin bones for females starting at 9.287 and the final observed mean of 9.281 resulting in almost no change in the mean. For males, the average number of dorsal fin bones at the first time point was about 9.568 dropping to 9.734 over the course of the observed time periods for a gain of 0.166 bones on average.

time	cle	ds1	ds2	ds3	ect	lps	lpt	maf	mav	mcv	mdf	pmx	stl
1	0.913	0.215	0.359	0.203	0.865	0.428	0.853	0.944	0.391	0.507	0.959	0.948	0.883
2	0.942	0.212	0.325	0.180	0.891	0.404	0.853	0.948	0.520	0.520	0.963	0.967	0.908
3	0.843	0.207	0.249	0.153	0.770	0.279	0.803	0.965	0.289	0.525	0.977	0.912	0.777
4	0.890	0.210	0.249	0.201	0.830	0.372	0.741	0.977	0.435	0.589	0.986	0.935	0.831
5	0.954	0.211	0.211	0.195	0.909	0.377	0.756	0.985	0.533	0.622	0.992	0.975	0.921
6	0.885	0.211	0.134	0.171	0.820	0.291	0.686	0.991	0.645	0.456	0.996	0.949	0.811
7	0.812	0.211	0.124	0.239	0.760	0.340	0.617	0.994	0.224	0.717	0.999	0.879	0.747
8	0.928	0.210	0.135	0.258	0.885	0.387	0.706	0.994	0.342	0.730	1.000	0.969	0.872
9	0.899	0.213	0.145	0.304	0.857	0.406	0.715	0.995	0.521	0.756	1.000	0.940	0.845
10	0.954	0.217	0.235	0.555	0.940	0.571	0.810	0.997	0.454	0.719	1.000	0.976	0.935
11	0.913	0.211	0.162	0.476	0.875	0.388	0.703	0.997	0.363	0.657	1.000	0.957	0.864
12	0.949	0.221	0.262	0.726	0.929	0.585	0.803	0.997	0.462	0.595	1.000	0.968	0.926
13	0.904	0.220	0.260	0.789	0.885	0.598	0.795	0.998	0.470	0.370	1.000	0.929	0.872
14	0.925	0.220	0.280	0.883	0.906	0.659	0.854	0.997	0.526	0.472	1.000	0.958	0.898
15	0.880	0.225	0.283	0.839	0.849	0.617	0.796	0.997	0.490	0.398	1.000	0.919	0.834

time	cle	ds1	ds2	ds3	ect	lps	lpt	maf	mav	mcv	mdf	pmx	stl
16	0.953	0.216	0.276	0.931	0.931	0.614	0.831	0.997	0.414	0.541	1.000	0.975	0.925
17	0.803	0.219	0.232	0.832	0.765	0.383	0.655	0.996	0.569	0.758	1.000	0.854	0.751
18	0.780	0.212	0.225	0.817	0.726	0.297	0.558	0.995	0.705	0.722	0.999	0.859	0.717

time	cle	ds1	ds2	ds3	ect	lps	lpt	maf	mav	mcv	mdf	pmx	stl
1	0.500	0.500	0.500	0.500	0.500	0.500	0.500	0.500	0.500	0.500	0.500	0.500	0.500
2	0.514	0.504	0.509	0.495	0.512	0.508	0.517	0.495	0.396	0.490	0.495	0.511	0.513
3	0.636	0.514	0.559	0.516	0.628	0.601	0.602	0.475	0.523	0.480	0.476	0.626	0.641
4	0.563	0.509	0.544	0.459	0.558	0.539	0.672	0.456	0.436	0.450	0.458	0.556	0.562
5	0.543	0.507	0.551	0.417	0.539	0.522	0.687	0.436	0.389	0.425	0.439	0.537	0.544
6	0.618	0.512	0.589	0.415	0.613	0.579	0.716	0.415	0.317	0.522	0.419	0.612	0.620
7	0.591	0.510	0.601	0.364	0.589	0.564	0.712	0.379	0.546	0.382	0.383	0.588	0.592
8	0.539	0.507	0.579	0.324	0.536	0.514	0.683	0.373	0.478	0.368	0.378	0.537	0.540
9	0.524	0.506	0.586	0.299	0.521	0.510	0.636	0.355	0.408	0.340	0.359	0.523	0.522
10	0.379	0.497	0.544	0.203	0.377	0.400	0.578	0.321	0.438	0.359	0.324	0.385	0.373
11	0.531	0.508	0.605	0.226	0.528	0.517	0.685	0.301	0.528	0.403	0.303	0.530	0.533
12	0.363	0.492	0.547	0.150	0.360	0.386	0.566	0.284	0.439	0.436	0.284	0.369	0.358
13	0.373	0.495	0.555	0.133	0.372	0.386	0.561	0.269	0.432	0.575	0.268	0.378	0.371
14	0.326	0.496	0.548	0.102	0.326	0.349	0.514	0.255	0.399	0.514	0.253	0.334	0.323
15	0.365	0.492	0.552	0.107	0.365	0.373	0.502	0.250	0.433	0.554	0.247	0.368	0.367
16	0.361	0.497	0.574	0.084	0.360	0.381	0.570	0.234	0.462	0.463	0.229	0.369	0.356
17	0.561	0.504	0.629	0.116	0.559	0.542	0.669	0.226	0.364	0.313	0.219	0.559	0.565
18	0.625	0.512	0.648	0.121	0.617	0.596	0.735	0.220	0.281	0.356	0.212	0.622	0.627

6 Discsusson, Future work and conclusions

We predicted that release from predators would result in niche expansion and increased sexual dimorphism, based on several studies of modern stickleback. For example, in lakes where sculpin competitors are absent and stickleback (Roesti et al. 2023) See Spoljaric and Reimchen 2008, page 512 right column for references and discussion of differences between benthic males and limnetic females. Male stickleback are benthic and littoral (Wootton 1976).... Reimchen papers in general good for this section.

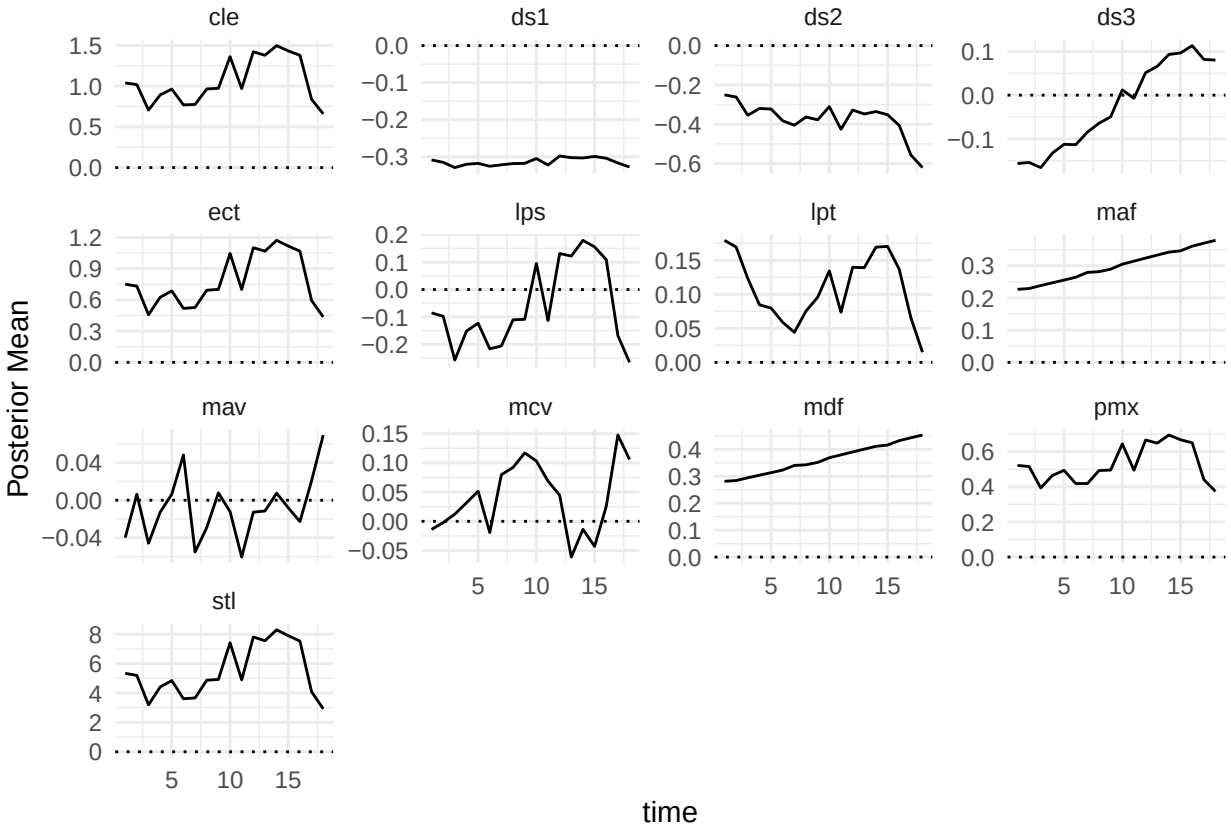

Figure 2: Posterior mean difference between males and females

Acknowledgements

We thank O. Abughoush, S. Blaine, A. Chaudhary, M. Islam, F. Joaquin, C. Lawson-Weinert, R. Sullivan, J. Tien, M.P. Travis, and W. Shim for help with data collection. We thank D. Schluter and S. Blain for loaning specimens and sharing data. We thank K. Swagel and C. McMahan of the Field Museum for assistance with specimen x-rays. This research was supported by NSF grants BSR-8111013, EAR-9870337, and DEB-0322818, the Center for Field Research (Earthwatch), and the National Geographic Society (2869-84) to MAB. It was also supported by NSF grants DEB-1456462 and EAR-2145830 to YES. And NSF DMS-2015374 (GJM)

Supplementary Material

All code for reproducing the analyses in this paper is publicly available at https://github.com/Akhil-Ghosh/SticklebackProject

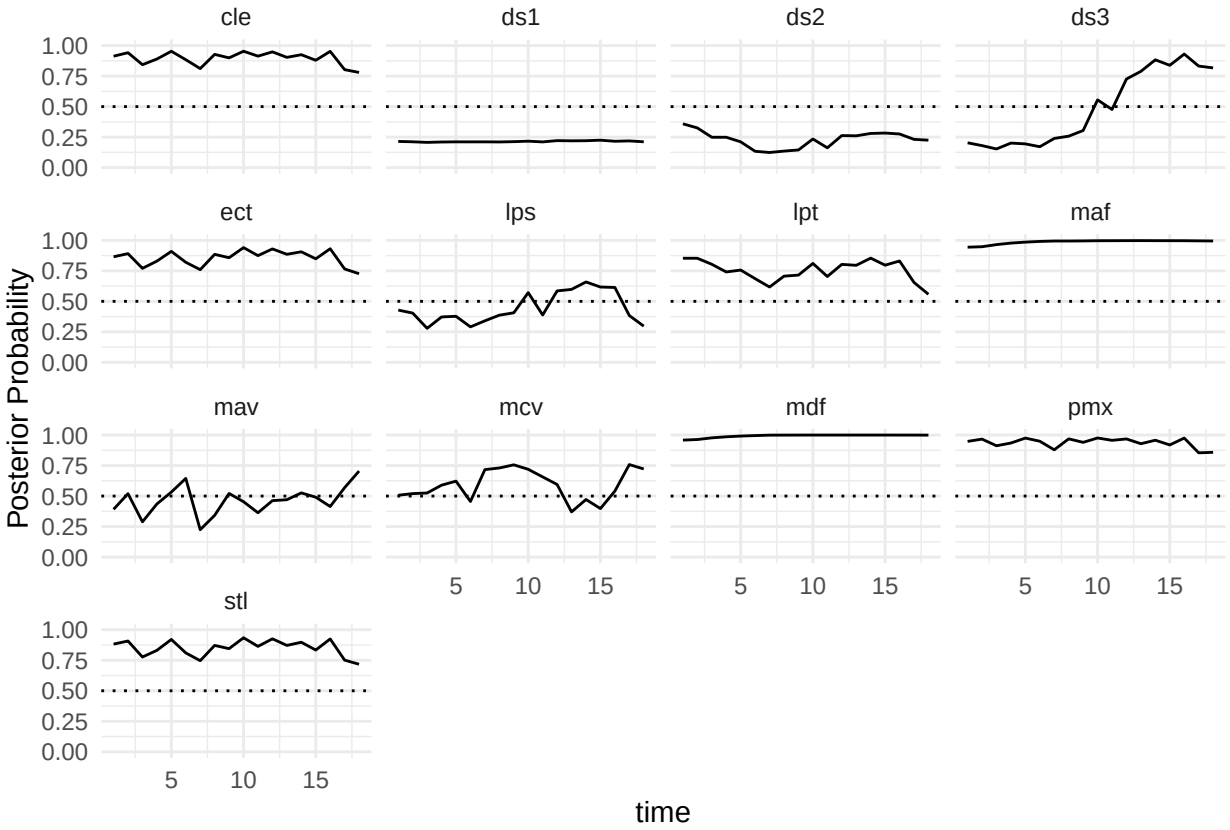

Figure 3: Posterior probabilities that mean for males is greater than mean for females

DIC results here.

6.1 Figures

References

Aguirre, Windsor E, Kendal Walker, and Shawn Gideon. 2014. "Tinkering with the Axial Skeleton: Vertebral Number Variation in Ecologically Divergent Threespine Stickleback Populations." *Biol. J. Linn. Soc. Lond.* 113 (1): 204–19.

Bell, M A. 2009. "Implications of a Fossil Stickleback Assemblage for Darwinian Gradualism." *J. Fish Biol.* 75 (8): 1977–99.

Bell, Michael A, Matthew P Travis, and D Max Blouw. 2006. "Inferring Natural Selection in a Fossil Threespine Stickleback." *Paleobiology* 32 (4): 562–77.

Bell, Orti, M. A., and J. P. Koenings. 1993. "Evolution of Pelvic Reduction in Threespine Sticklebacks: A Test of Competing Hypotheses." *Evolution* 47: 906–14.

Blain, S A. 2022. *Evolutionary Outcomes of Interactions Among Phenotypes in Post-Glacial*

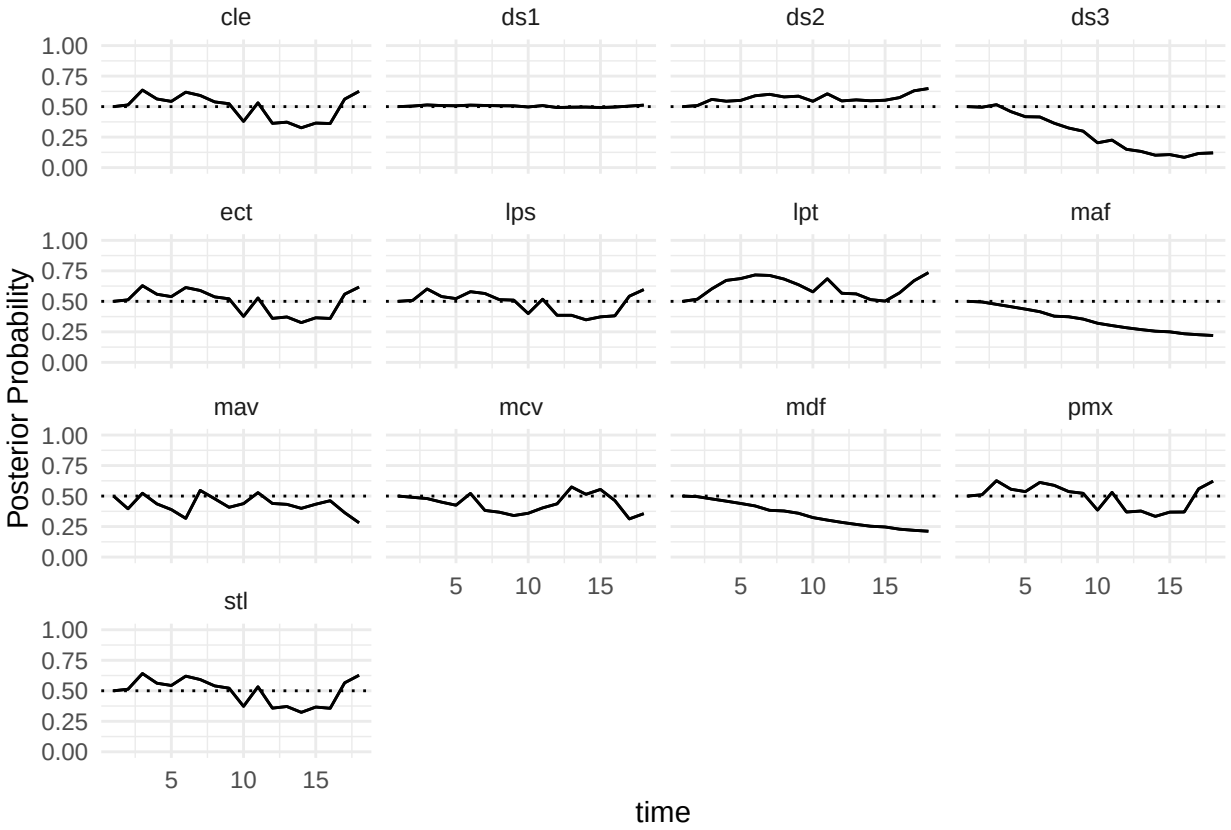

Figure 4: AUC comparing time x versus time 0.

Lakes. University of British Columbia, Canada.

Bolnick, Daniel I. 2011. "Sympatric Speciation in Threespine Stickleback: Why Not?" *Int. J. Ecol.* 2011: 1–15.

Bolnick, Daniel I, and Michael Doebeli. 2003. "Sexual Dimorphism and Adaptive Speciation: Two Sides of the Same Ecological Coin." *Evolution* 57 (11): 2433–49.

Bolnick, Daniel I, Travis Ingram, William E Stutz, Lisa K Snowberg, On Lee Lau, and Jeff S Paull. 2010. "Ecological Release from Interspecific Competition Leads to Decoupled Changes in Population and Individual Niche Width." *Proc. Biol. Sci.* 277 (1689): 1789–97.

Bolnick, Daniel I, and On Lee Lau. 2008. "Predictable Patterns of Disruptive Selection in Stickleback in Postglacial Lakes." *Am. Nat.* 172 (1): 1–11.

Bowne, P S. 1994. "Systematics and Morphology of the Gasterosteiformes." In *The Evolutionary Biology of the Threespine Stickleback*, edited by M A Bell and S A Foster. Oxford, UK: Oxford University Press.

Butler, Marguerite A, Stanley A Sawyer, and Jonathan B Losos. 2007. "Sexual Dimorphism and Adaptive Radiation in Anolis Lizards." *Nature* 447 (7141): 202–5.

Buuren, Stef van, and Karin Groothuis-Oudshoorn. 2011. "Mice: Multivariate Imputation by Chained Equations in r." *Journal of Statistical Software* 45 (3): 1–67. https://doi.org/10.18637/jss.v045.i03.

Cooper, Idelle A, R Tucker Gilman, and Janette Wenrick Boughman. 2011. "Sexual Dimorphism and Speciation on Two Ecological Coins: Patterns from Nature and Theoretical Predictions." *Evolution* 65 (9): 2553–71.

Cornuault, Josselin. 2022. "Bayesian Analyses of Comparative Data with the Ornstein–Uhlenbeck Model: Potential Pitfalls." *Systematic Biology* 71 (6): 1524–40. https://doi.org/10.1093/sysbio/syac036.

De Lisle, S. Paiva, S. P., and L. Rowe. 2018. "Habitat Partitioning During Character Displacement Between the Sexes." *Biology Letters* 14: 20180124.

De Lisle, S. P., and L. Rowe. 2015. "Ecological Character Displacement Between the Sexes." *The American Naturalist* 186: 693–707.

Hendry, A P, D I Bolnick, D Berner, and C L Peichel. 2009. "Along the Speciation Continuum in Sticklebacks." *J. Fish Biol.* 75 (8): 2000–2036.

Herrmann, Nicholas C, James T Stroud, and Jonathan B Losos. 2021. "The Evolution of 'Ecological Release' into the 21st Century." *Trends Ecol. Evol.* 36 (3): 206–15.

Hone, David W E, and Jordan C Mallon. 2017. "Protracted Growth Impedes the Detection of Sexual Dimorphism in Non-Avian Dinosaurs." *Palaeontology* 60 (4): 535–45.

Hunt, Gene, Michael A Bell, and Matthew P Travis. 2008. "Evolution Toward a New Adaptive Optimum: Phenotypic Evolution in a Fossil Stickleback Lineage." *Evolution* 62 (3): 700–710.

Little, R. J. A., and D. B. Rubin. 2002. *Statistical Analysis with Missing Data*. Wiley Series in Probability and Mathematical Statistics. Probability and Mathematical Statistics. Wiley. http://books.google.com/books?id=aYPwAAAAMAAJ.

Reimchen, D. Steeves, T. E. 2016. "Sex Matters for Defence and Trophic Traits of Threespine Stickleback." *Evolutionary Ecology Research* 17: 459-485-.

Reimchen, T. E. 1980. "Spine Deficiency and Polymorphism in a Poulation of Gasterosteus Aculeatus: An Adaptation to Predators?" *Canadian Journal of Zoology* 58: 1232–44.

———. 1994. "Predators and Morphological Evolution in Threespine Stickleback." In *The Evolutionary Biology of the Threespine Stickleback*, edited by M A Bell and S A Foster. Oxford, UK: Oxford University Press.

Reimchen, T. E., and P. Nosil. 2004. "Variable Predation Regimes Predict the Evolution of Sexual Dimorphism in a Population of Threespine Stickleback." *Evolution* 58 (6): 1274–81.

Roesti, J. S. Groh, M, and D. Schluter. 2023. "Species Divergence Under Competition and Shared Predation." *Ecology Letters* 26: 111–23.

Saitta, Evan T, Maximilian T Stockdale, Nicholas R Longrich, Vincent Bonhomme, Michael J Benton, Innes C Cuthill, and Peter J Makovicky. 2020. "An Effect Size Statisti-

cal Framework for Investigating Sexual Dimorphism in Non-Avian Dinosaurs and Other Extinct Taxa." *Biological Journal of the Linnean Society* 131 (2): 231–73. https://doi.org/10.1093/biolinnean/blaa105.

Schluter, D, and J D McPhail. 1992. "Ecological Character Displacement and Speciation in Sticklebacks." *Am. Nat.* 140 (1): 85–108.

Shine, R. 1989. "Ecological Causes for the Evolution of Sexual Dimorphism: A Review of the Evidence." *Q. Rev. Biol.* 64 (4): 419–61.

Spoljaric, M. A., and T. E. Reimchen. 2008. "Habitat-Dependent Reduction of Sexual Dimorphism in Geometric Body Shape of Haida Gwaii Threespine Stickleback." *Biological Journal of the Linnean Society* 95: 505–16.

Stuart, Yoel E, J William Sherwin, Ambika Kamath, and Thor Veen. 2021. "Male and Female Anolis Carolinensis Maintain Their Dimorphism Despite the Presence of Novel Interspecific Competition." *Evolution* 75 (11): 2708–16.

Stuart, Yoel E, Matthew P Travis, and Michael A Bell. 2020. "Inferred Genetic Architecture Underlying Evolution in a Fossil Stickleback Lineage." *Nat. Ecol. Evol.* 4 (11): 1549–57.

Stuart, Yoel E, Thor Veen, Jesse N Weber, Dieta Hanson, Mark Ravinet, Brian K Lohman, Cole J Thompson, et al. 2017. "Contrasting Effects of Environment and Genetics Generate a Continuum of Parallel Evolution." *Nat. Ecol. Evol.* 1 (6): 158.

Team, R Core. 2022. *R: A Language and Environment for Statistical Computing*. Vienna, Austria: R Foundation for Statistical Computing. https://www.R-project.org/.

Uhlenbeck, G. E., and L. S. Ornstein. 1930. "On the Theory of the Brownian Motion." *Phys. Rev.* 36 (September): 823–41. https://doi.org/10.1103/PhysRev.36.823.

Voje, Kjetil L, Michael A Bell, and Yoel E Stuart. 2022. "Evolution of Static Allometry and Constraint on Evolutionary Allometry in a Fossil Stickleback." *J. Evol. Biol.* 35 (3): 423–38.

W., Schoener T. 1968. "The Anolis Lizards of Bimini: Resource Partitioning in a Complex Fauna." *Ecology* 49: 704–26.

Zhou, X., and J. Reiter. 2010. "A Note on Bayesian Inference After Multiple Imputation." *The American Statistician* 64 (2): 159–63.

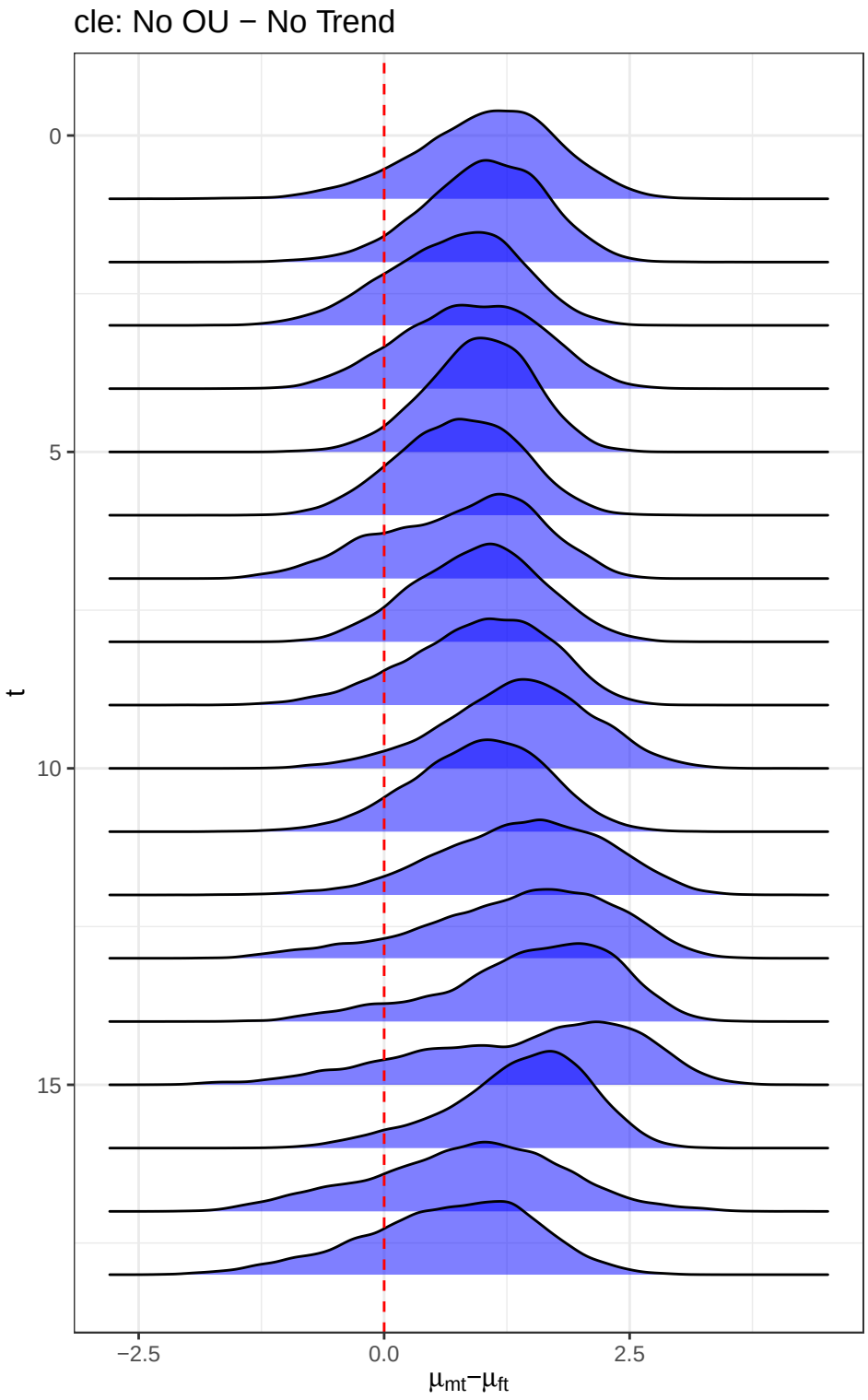

Figure 5: cle

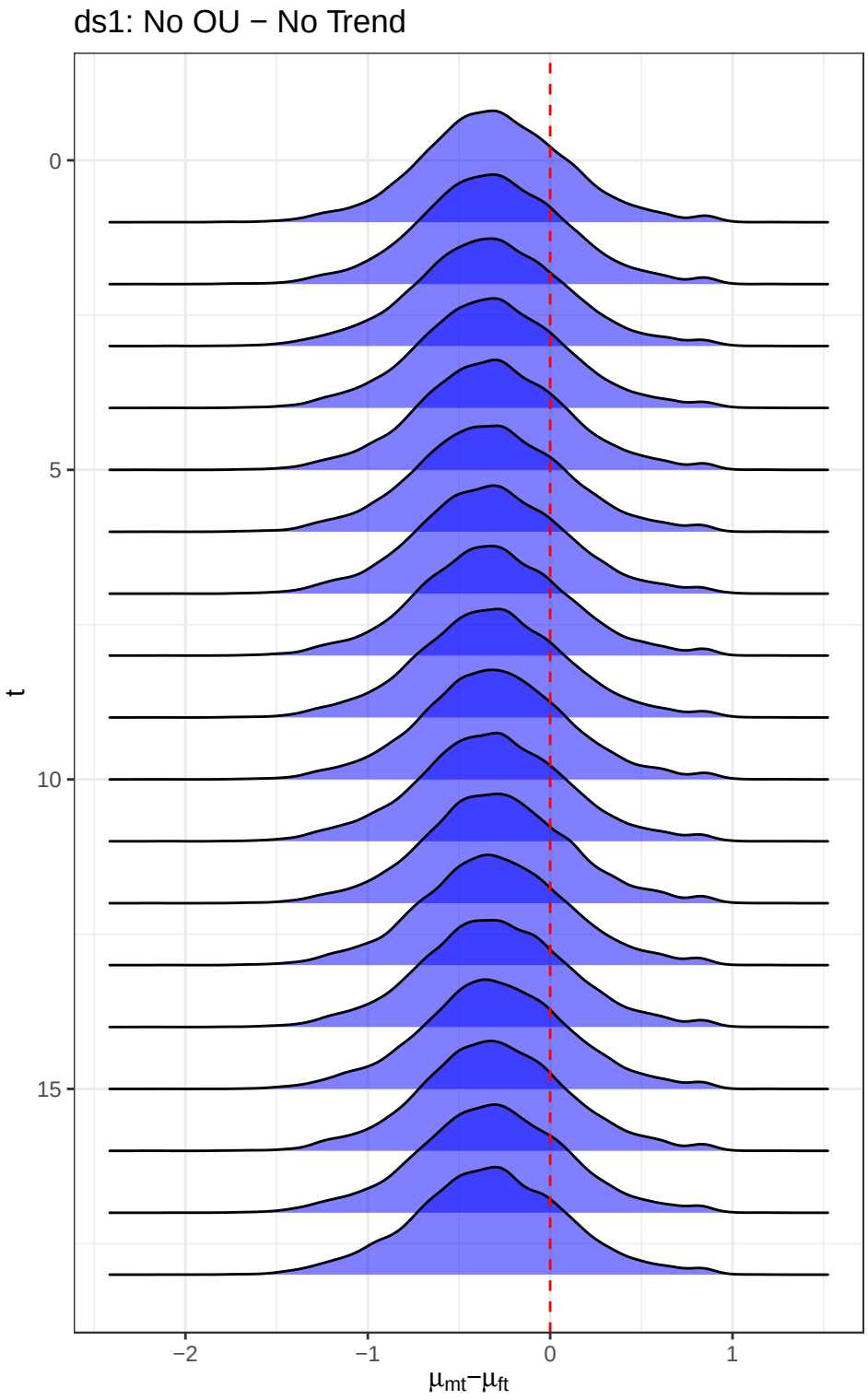

Figure 6: ds1

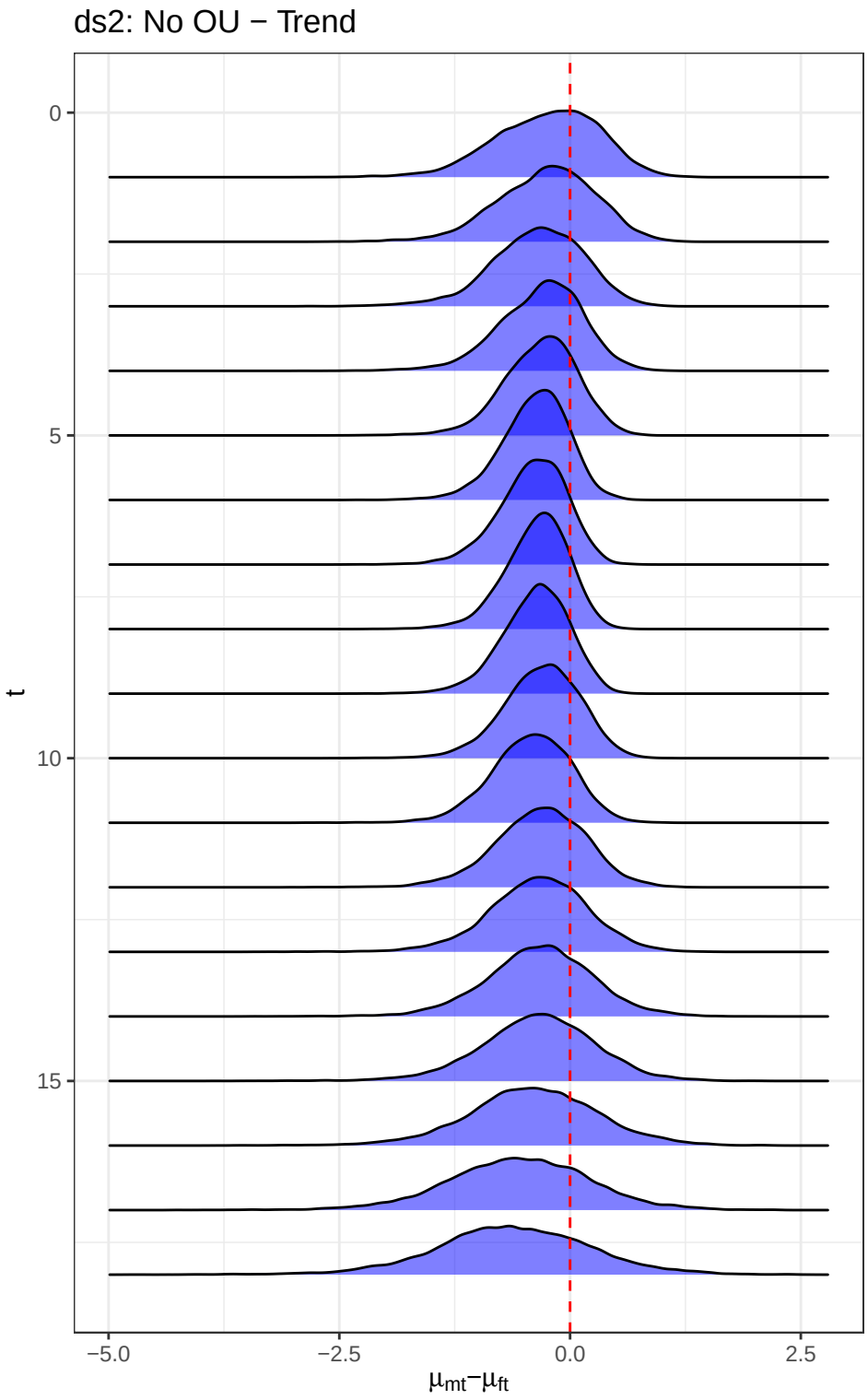

Figure 7: ds2

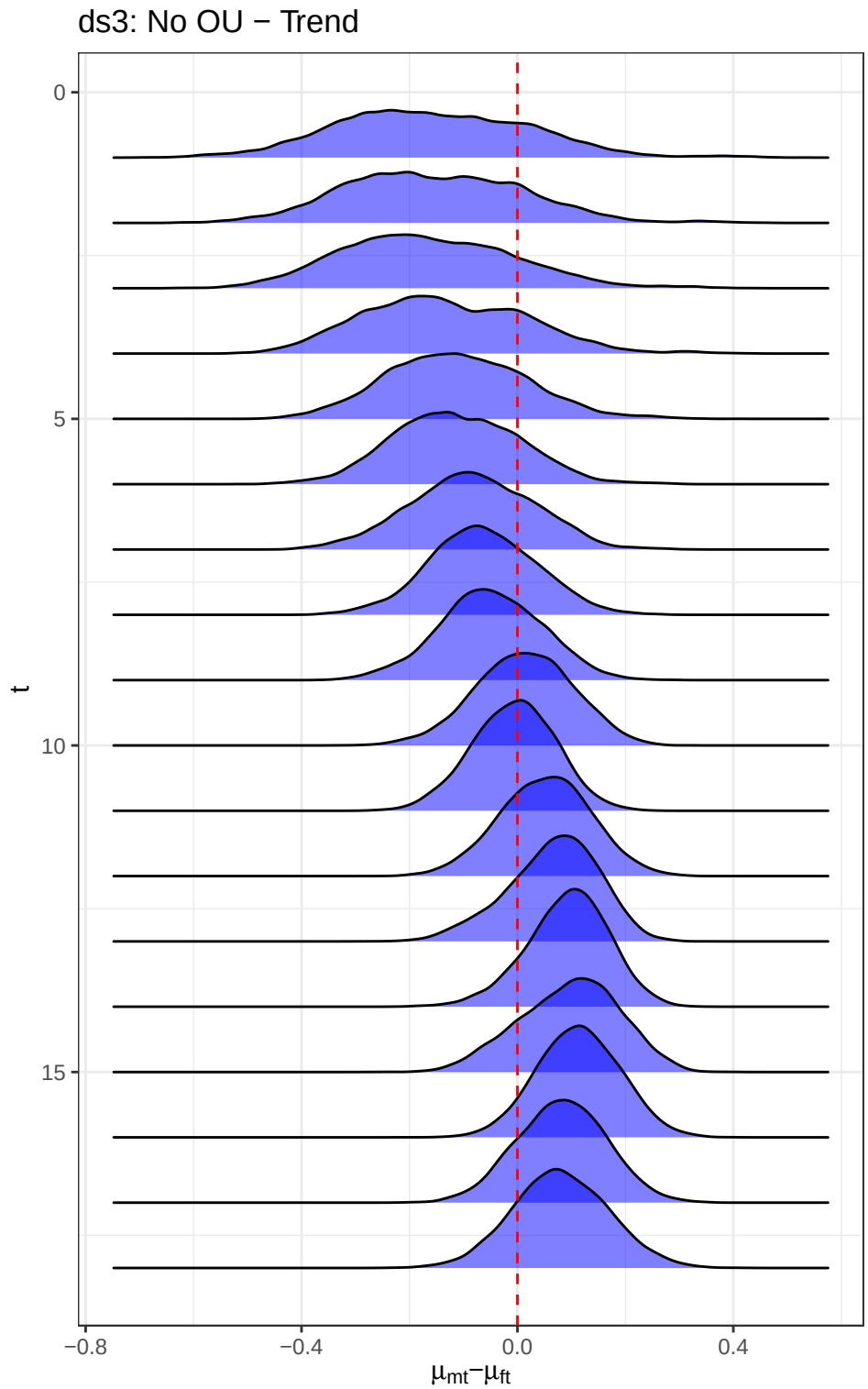

Figure 8: ds3

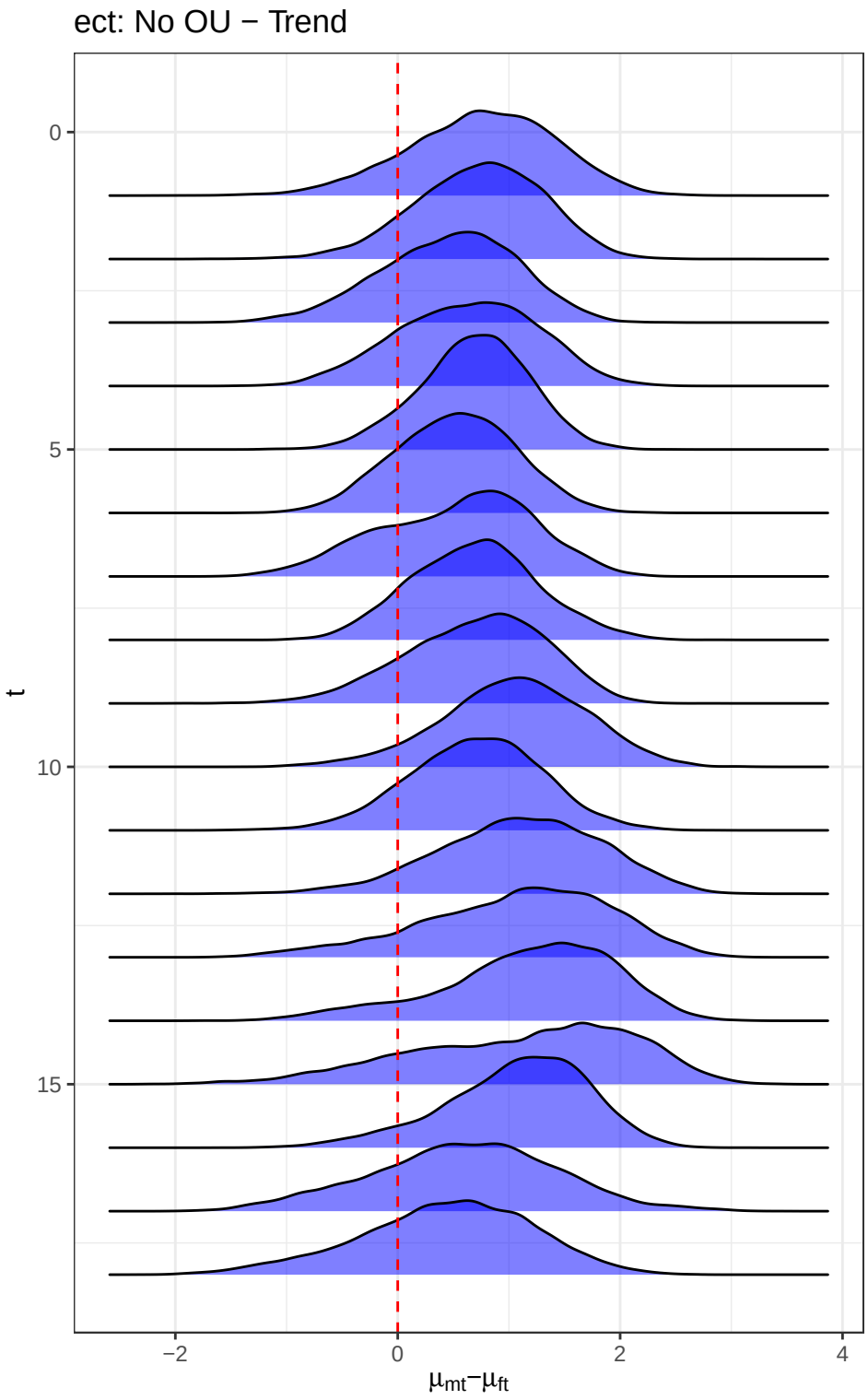

Figure 9: ect

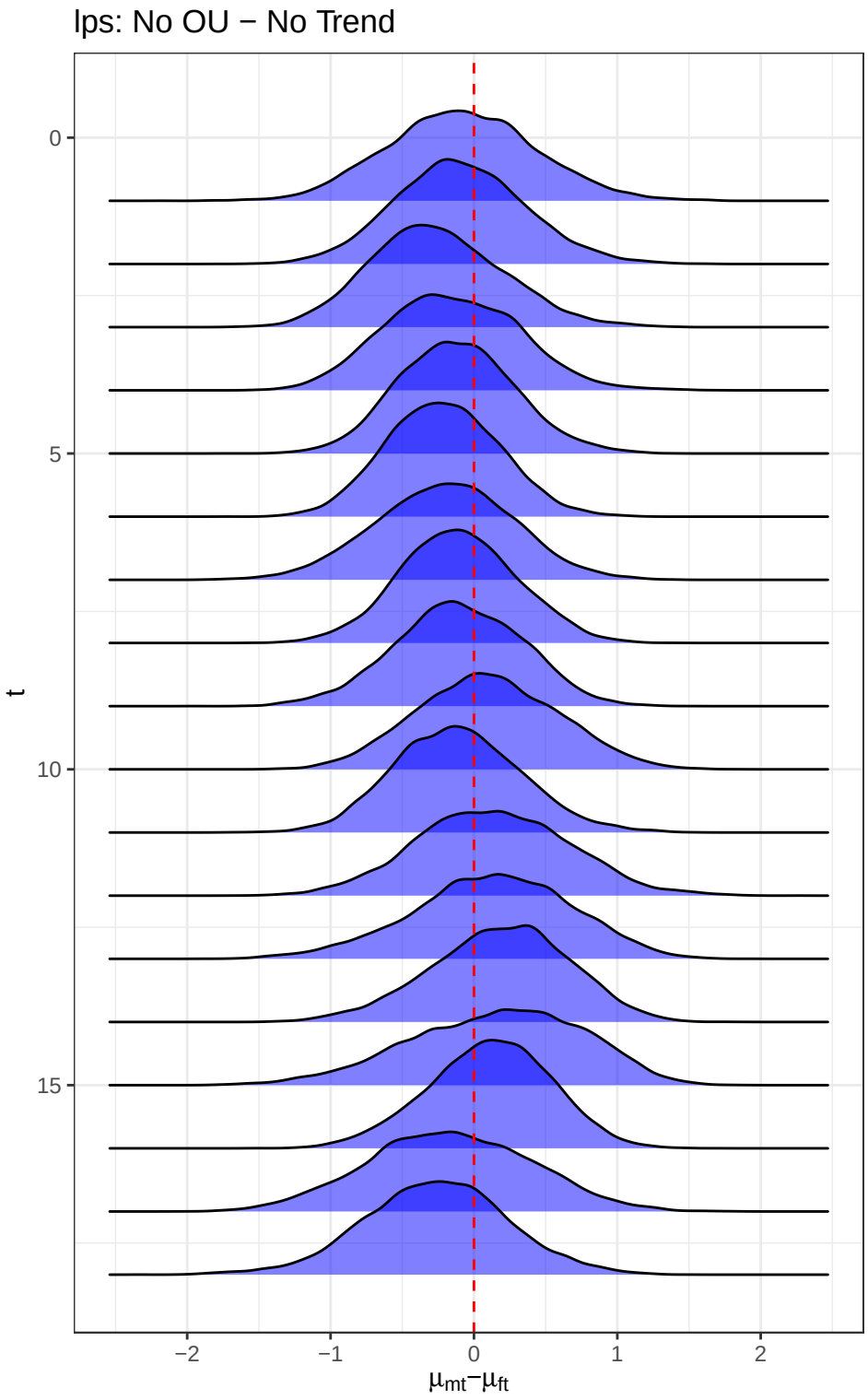

Figure 10: lps

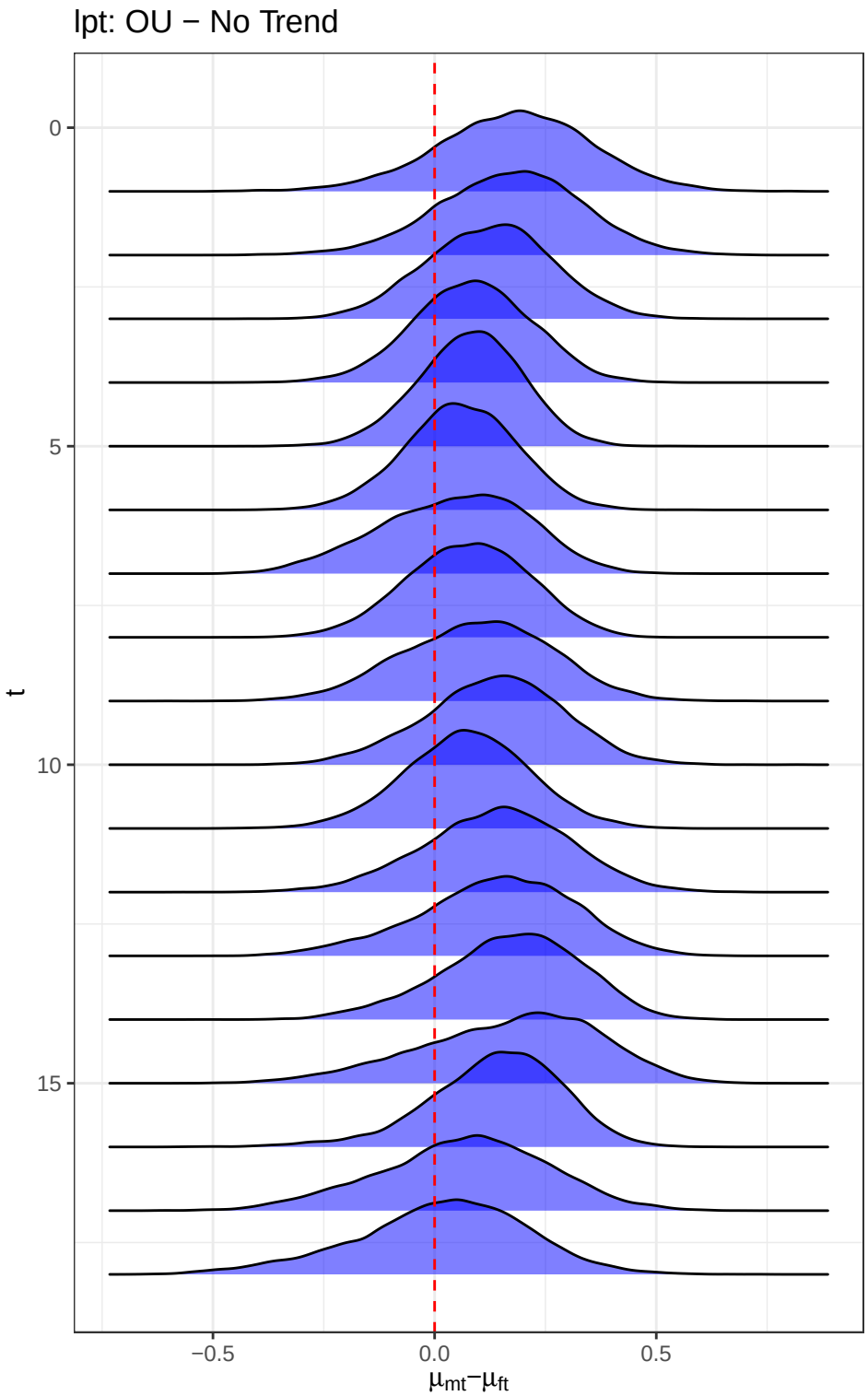

Figure 11: lpt

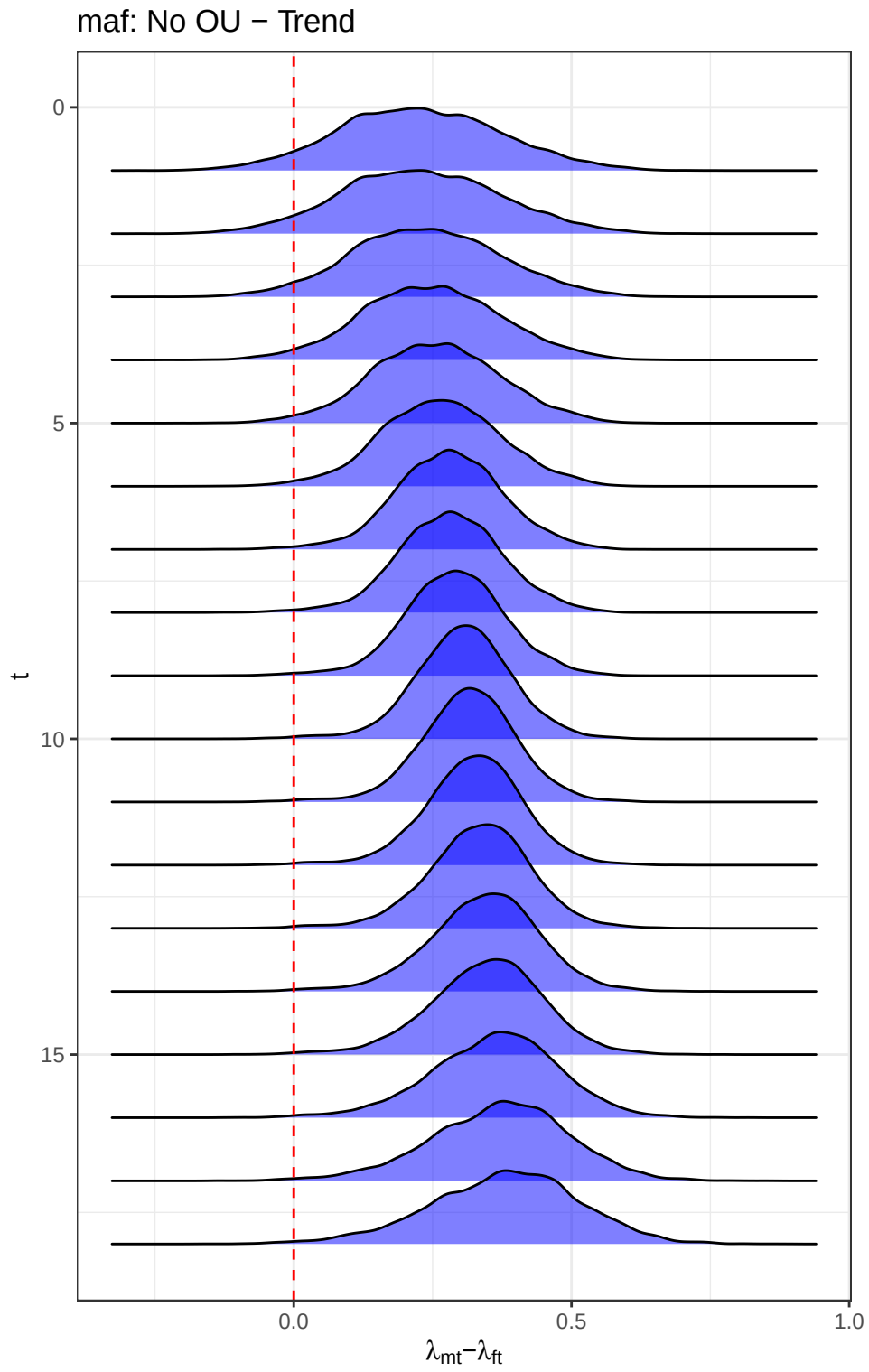

Figure 12: maf

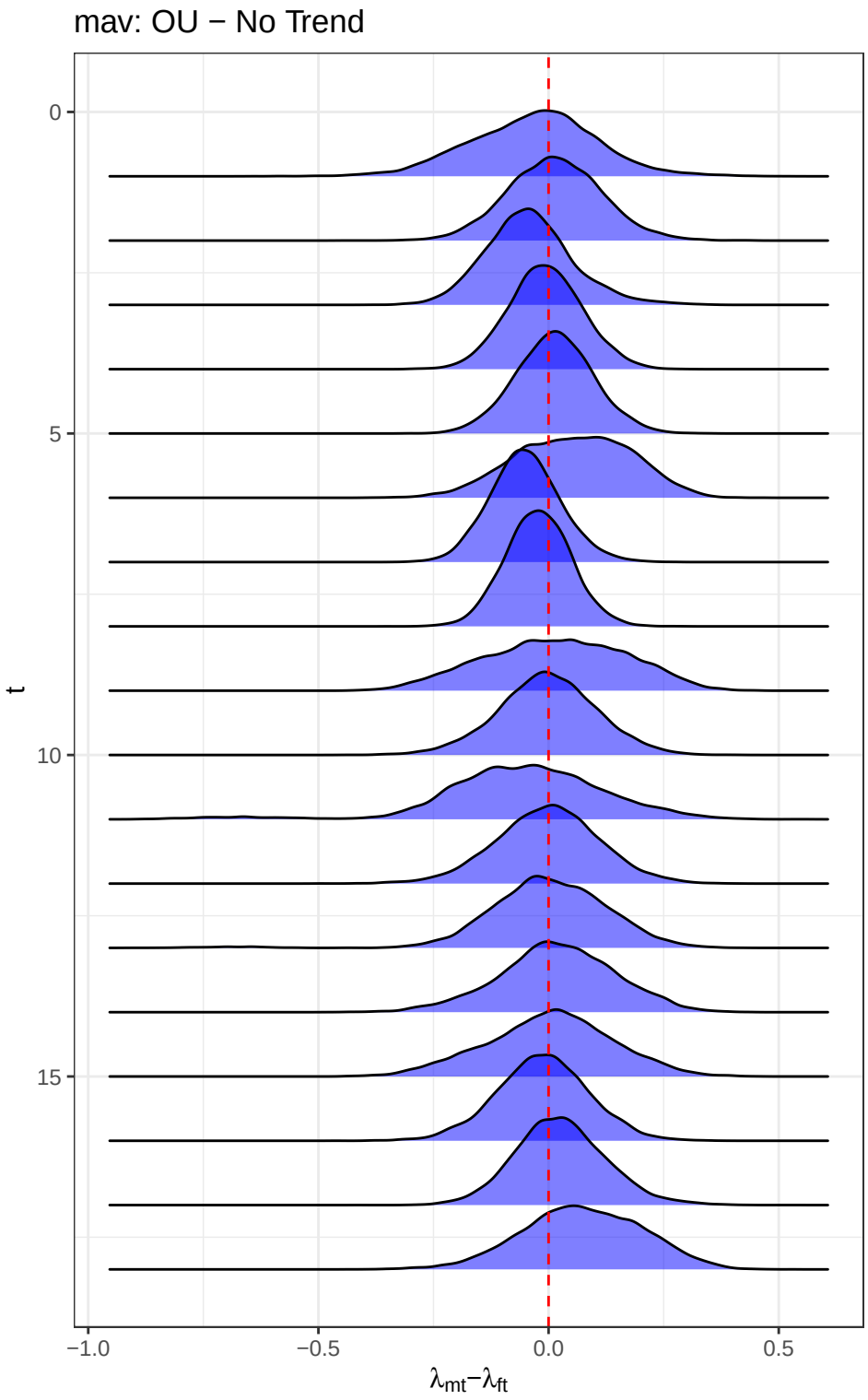

Figure 13: mav

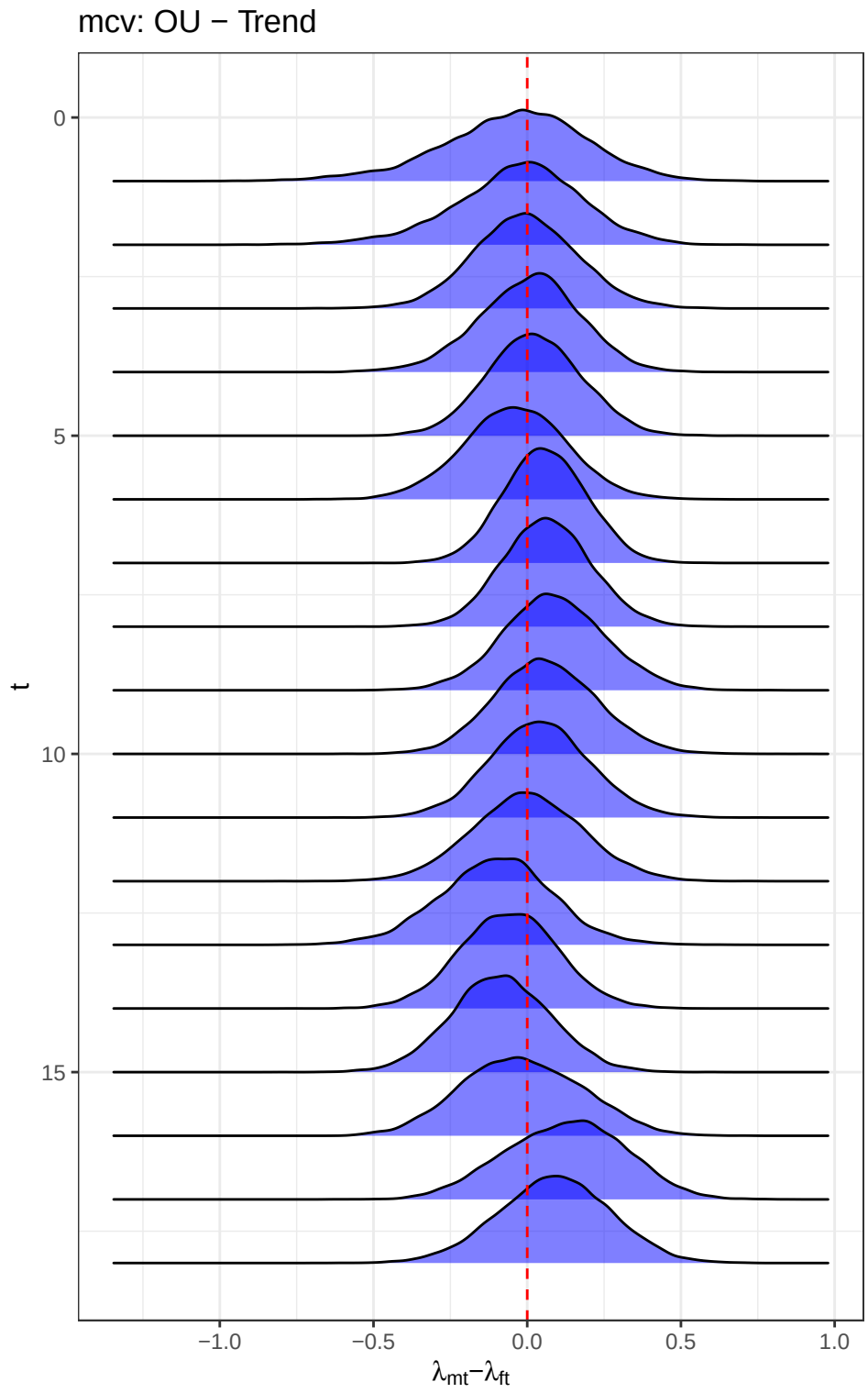

Figure 14: mcv

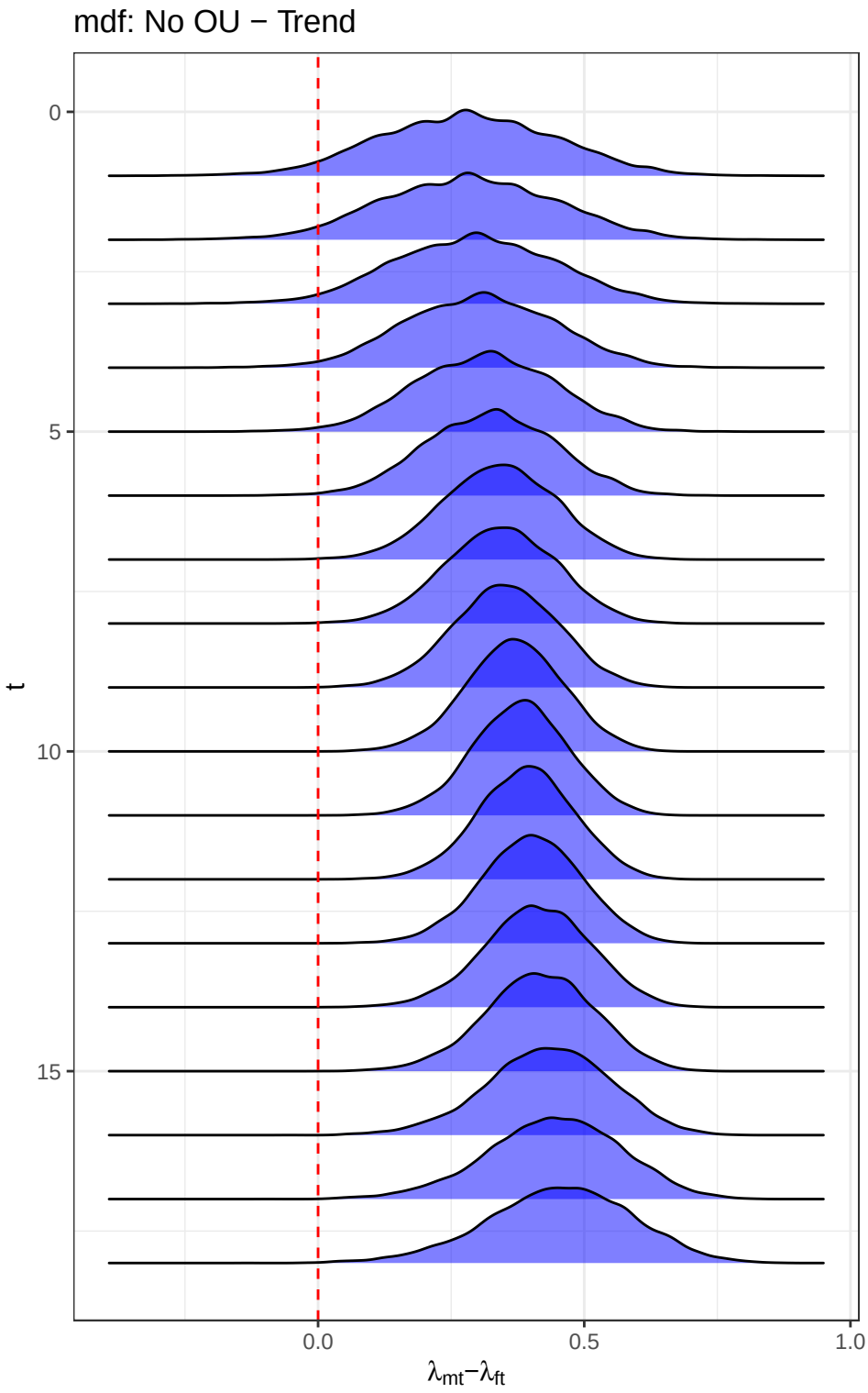

Figure 15: mdf

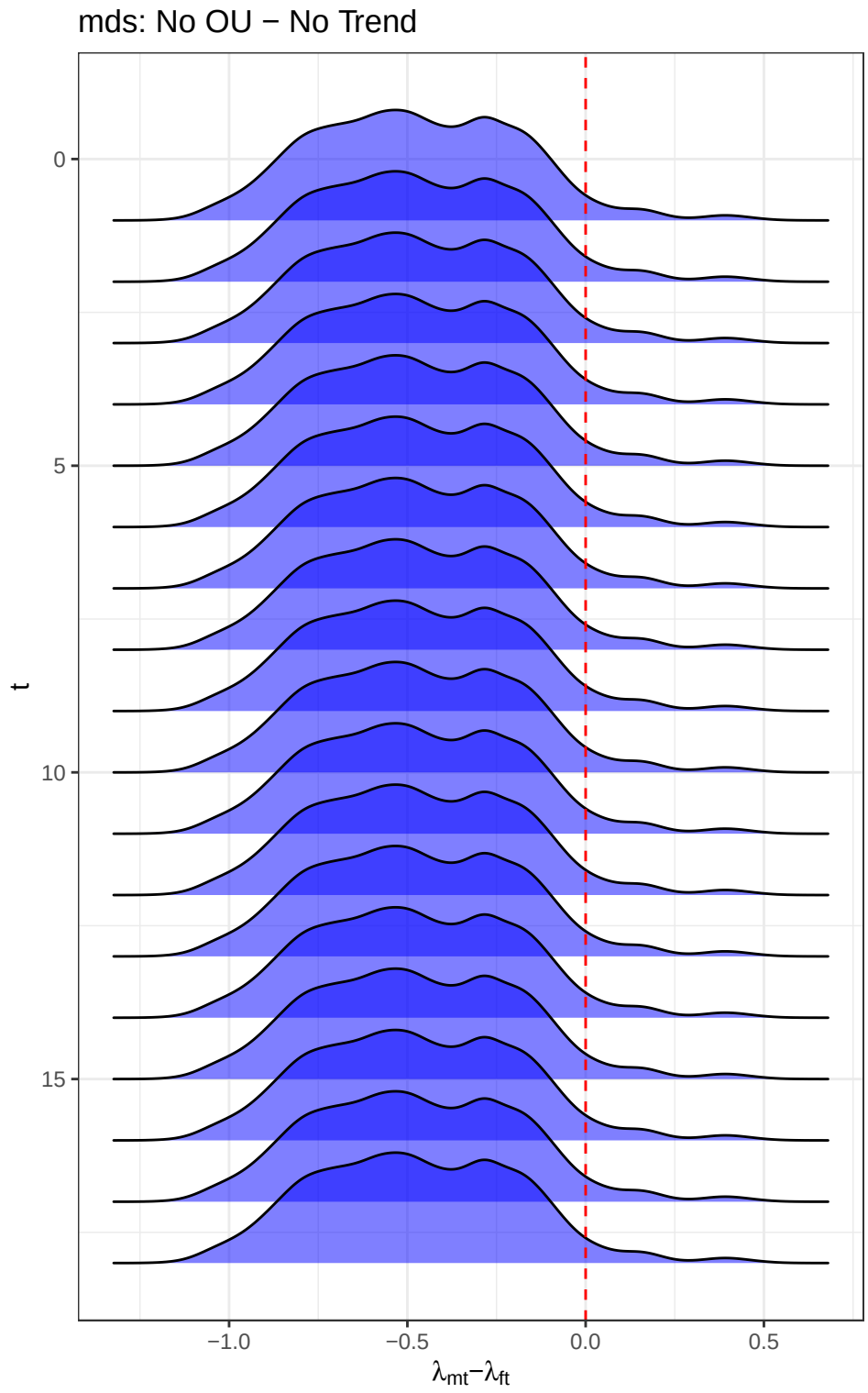

Figure 16: mds

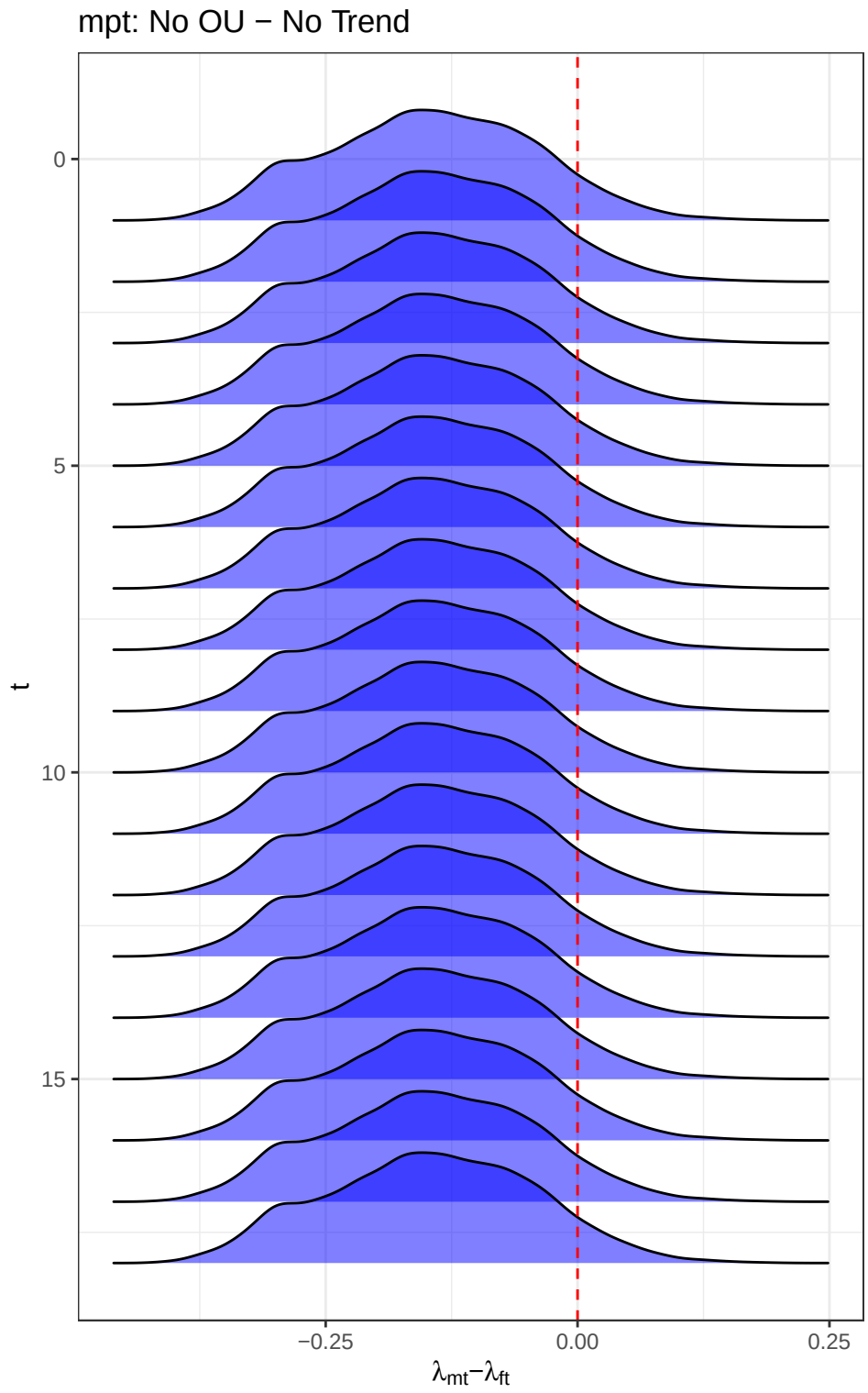

Figure 17: mpt

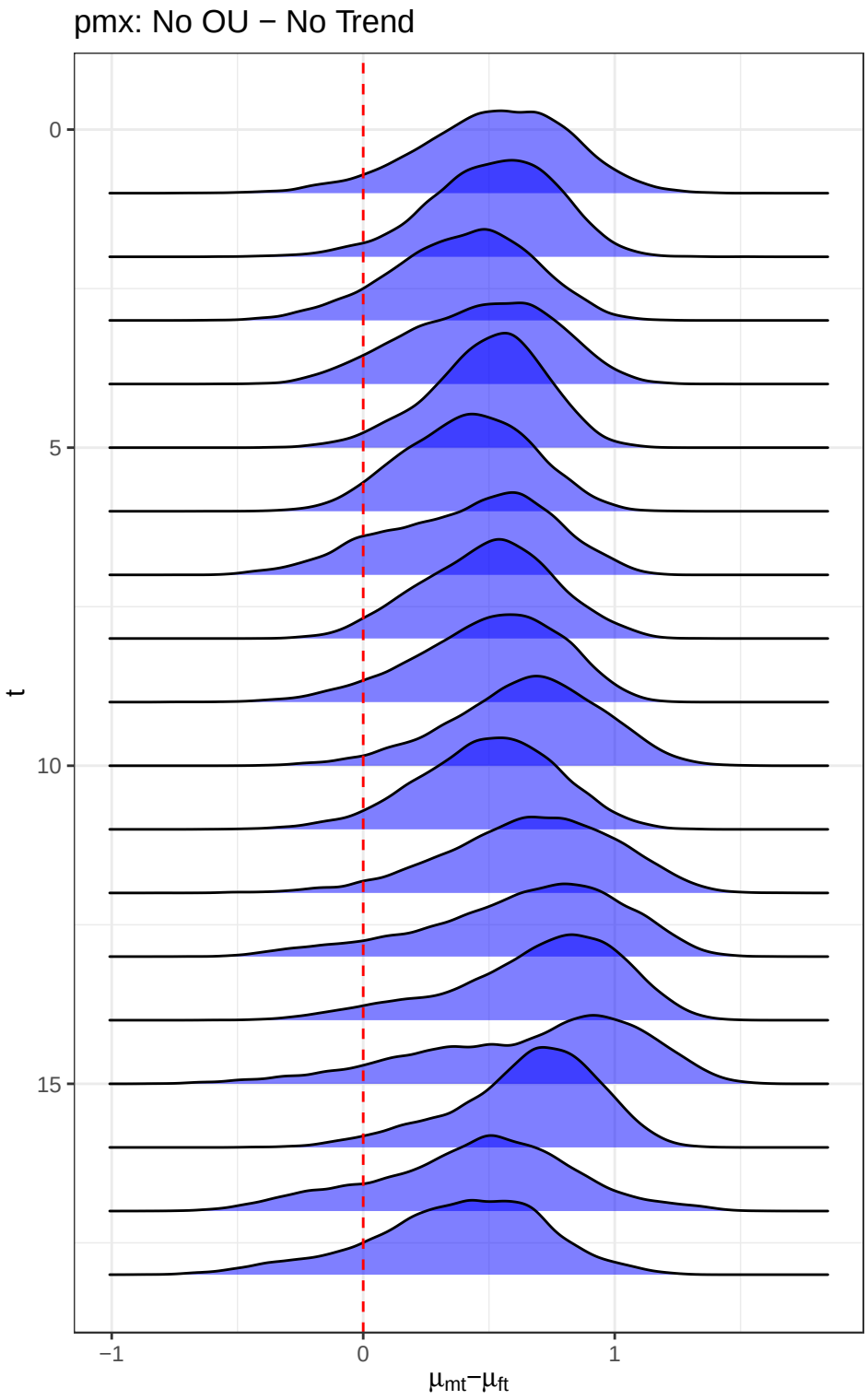

Figure 18: pmx

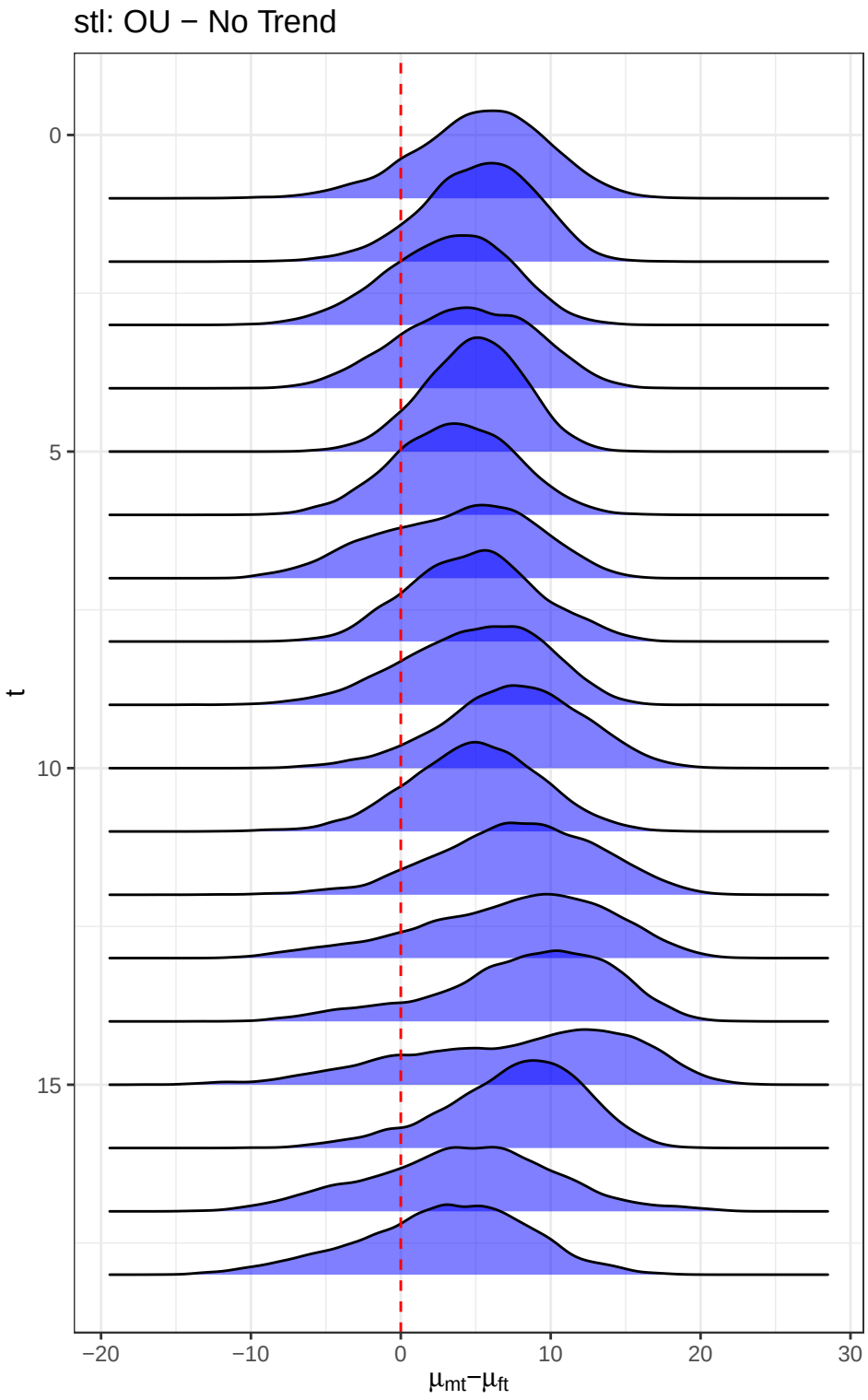

Figure 19: stl